

# PREDIS

## **PREDIS Final Conference - WP4 Innovations in metallic radioactive waste management**

---

**A. ABDELOUAS**

**ON BEHALF OF WP4 CONSORTIUM**

**05 JUNE 2024**



This project has received funding from the Euratom research and training programme 2019-2020 under grant agreement No 945098.



This project has received funding from the Euratom research and training programme 2019-2020 under grant agreement No 945098.

# Presentations

---

- Summary (Abdesselam Abdelouas – IMT Atlantique)
- Scientific presentations:
  - Developing and optimizing decontamination processes (T. Suzuki, MT Atlantique)
  - Optimization of characterization and waste minimization techniques (A. Savidou, NCSR D)
  - Advances in encapsulation of materials in magnesium phosphate cement-based matrices (C. Cannes, IJCLab)
- Students presentations:
  - A non-destructive gamma spectrometry set-up for characterization of metallic waste (D. Mavrikis, NCSR D)
  - Decontamination of radioactive effluents (M. Robin, IMT Atlantique)

# WP Objectives



- **Optimisation** and **innovation** for the management of large volumes of metallic waste (maintenance, dismantlement, etc...)
- **Characterisation techniques**
  - Non destructive control: classification & clearance
  - Difficult to measure radionuclides (RN): clearance
- **Decontamination techniques** mainly for recycling & clearance
- **Conditioning** of reactive metallic waste using innovative Magnesium Phosphate Cement (MPC) (Disposal)



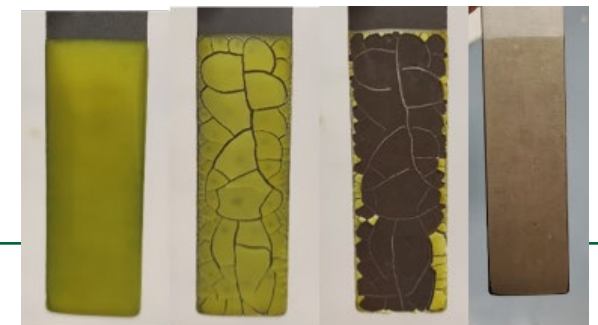
# WP Expected Impacts

---

- Making problematic metallic waste management routes (from storage to disposal) **safer** and more **economically efficient**.
- Contributing to repository use optimization, by allowing a more efficient use of the available disposal volumes (**recycling**).
- Reduction of waste management and disposal cost by valorization of part of the waste stream (**declassification, recycling, minimization**)

# Work Package 4 Structure

- Task 4.1 WP management (IMTA)
- Task 4.2 GAP analyses (IMTA, all)
- Task 4.3 Defining Europe-wide Needs and Opportunities for Management of Metallic Waste Streams (GSL)
- Task 4.4 Development and optimisation of decontamination processes (IMTA)
- Task 4.5 Optimisation of metallic waste characterisation and procedures for waste minimisation and recycling (NCSRD)
- Task 4.6 Encapsulation of reactive metals in magnesium phosphate cement-based matrices (CNRS)
- Task 4.7 Dissemination (IMTA)



13/06/2024

6

# WP Major Achievements, Task 4.4 Development and optimization of decontamination processes

---

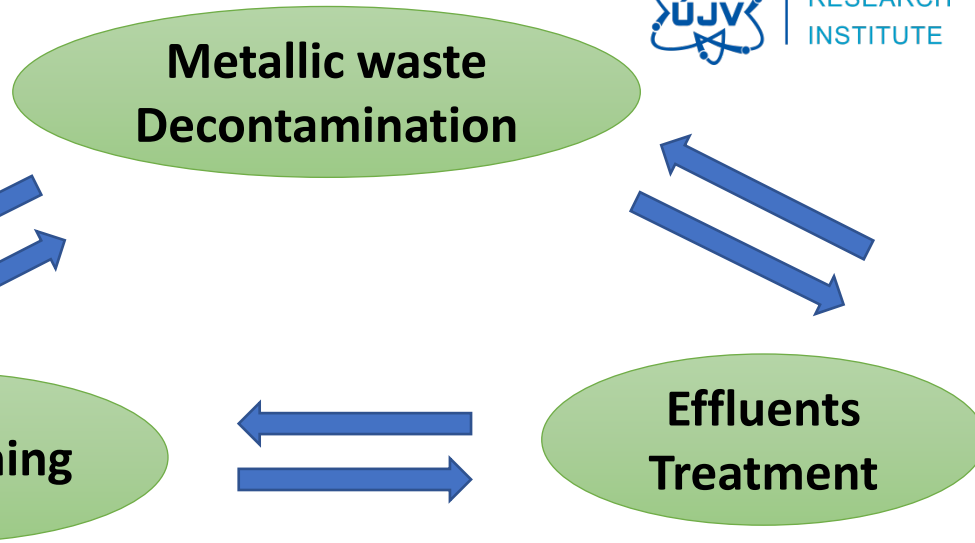
- **Optimization** of the CORD (Chemical Oxidation Reduction Decontamination) process.
- **COREMIX** (Chemical Oxidation Reduction using nitric permanganate and oxalic acid MIXture)

Aditya Rivonkar (2023) Optimization of chemical decontamination methods for radioactive metals. PhD Thesis, IMT Atlantique (France).

# WP Major Achievements, Task 4.4 optimization: COREMIX process



IMT Atlantique  
Bretagne-Pays de la Loire  
École Mines-Télécom



- Less complex process for industrial application: no UV light treatment for oxalic acid destruction. Safer, environmentally friendly & more economic !
  - Oxalic acid destruction by  $H_2O_2$  & heating. LCA/LCC approach helped optimizing the process by reducing energy consumption &  $CO_2$  production.
- Replacement of toxic and unstable permanganic acid ( $HMnO_4$ ) by a mixture of  $KMnO_4 + HNO_3$ .  $HMnO_4$  must be prepared onsite and requires expensive acid cation resins.
  - Safer, more environmentally friendly and more economic.
- Reduction of treatment time (less contact cycles) by 50%.
  - Safer, more environmentally friendly and more economic.
- The chemicals involved are compatible with the effluent treatment step as well as with the WAC for the conditioning/storage steps.
  - Use of chemical precipitation processes allowing the transformation of  $m^3$  of waste effluents into a few 100g of residues compatible with cement/geopolymer matrices (WP4 & WP5)



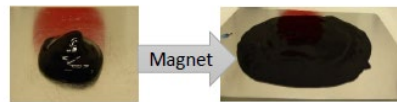
This project has received funding from the Euratom research and training programme 2019-2020 under grant agreement No 945098.

# WP Major Achievements, Task 4.4 innovation: magnetic gel decontamination

## Metallic waste Gel Decontamination

NATIONAL NUCLEAR LABORATORY

*Oxidized metal preparation  
Gel preparation & testing*



*Oxidized metal preparation*

- Development of gel formulations for “dry” decontamination
  - After drying the gel can be collected with the extracted contamination. No effluents: Safer, more environmentally friendly and more economic.
- Optimization of chemical parameters of the gel (e.g. COREMIX testing with gel).
  - Efficient for metals with small oxidized layer.
- Innovative formulation to decontaminate hardly accessible surfaces.
  - Gel application and removal using remotely a magnet.



*Gel preparation & testing*



IMT Atlantique  
Bretagne-Pays de la Loire  
École Mines-Télécom

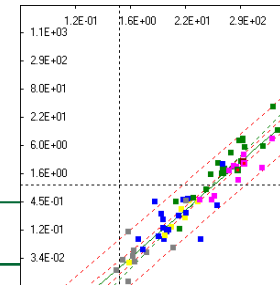
*COREMIX process testing*

# WP Major Achievements, Task 4.5 Optimization: radiological characterization



- Better determination of the waste management route
- Minimization of waste volume & increase of recycling

- Optimization of NDC using gamma spectrometry by reducing uncertainties.
  - Geometry of segment ; activity inhomogeneity ; measurement efficiency ; pipe direction
  - The method allows determination of activities of Cs-137 and Co-60 at the level of clearance in 1-2 min (amount of metallic waste about 100 kg)
  - Determination of activities in activated and / or contaminated metallic waste
- Optimization of sorting of metallic waste.
  - Scaling Factor.
- Development of procedures for DTM measurement.
  - Ni-59, Ni63, Mo-93, Ca-41, Zr-93
  - Validation will be held by an intercomparison exercise in 2024

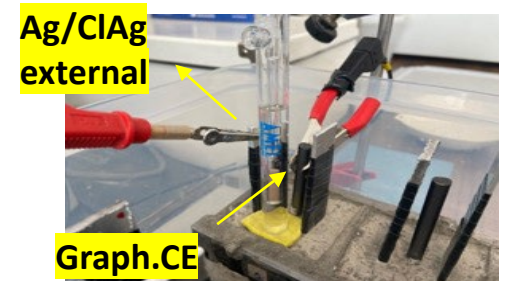
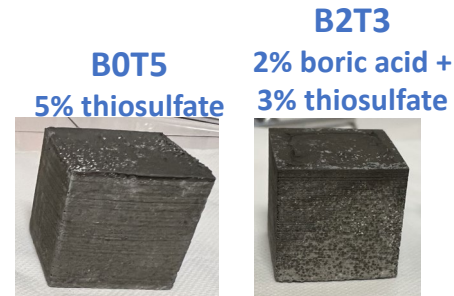


# WP Major Achievements, Task 4.6 Optimization: MPC formulations for reactive metallic waste encapsulation



- Development of magnesium phosphate cement formulations based on WAC and economical considerations.

- Development of MPC formulations
  - Testing new alternative fillers to replace fly ash (volcanic ash, wollastonite)
- Optimization of cost production
  - Replacement of dead burned MgO by reactive MgO + retarder. MPC price reduction by 15%.
  - Lowering the volume of cement and increase the volume of aggregates
- Qualification of the developed MPC formulations
  - Corrosion, irradiation of MPC-Al, MPC-carbon steel, beryllium



# Industrial support

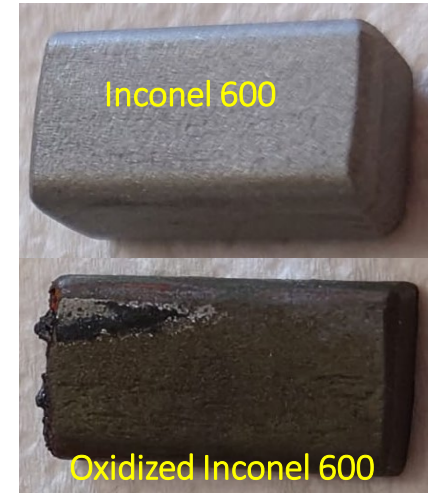
- Fruitful exchange with industrial partners
  - EDF, ORANO, ENRESA, ANDRA, Triskem...:
    - providing raw materials such as fly ash, metals (Ni-Alloy), resins
    - Advises in terms of suitable applications and processes, WAC, experimental conditions



Task 4.5



Task 4.6



Task 4.4

# Students involvement & Dissemination

- Number of PhD theses supported: **15**
  - Task 4: **8** (A. Rivonkar, M. Robin, T. Prasek, K. Fenclova, D. Barton, H. Lane, A. Santi, O. Ileri)
  - Task 5: **4** (A. Markopoulos, D. Mavrikis, E. Ntalla)
  - Task 6: **3** (M. Dieguez, I. Moschetti, C. Fernandez)
- MSc students: **8**
- Number of open access publications: Achieved: **9** ; Submitted: **6**
- Number of participation to workshops / conferences: **31**
- Number of Patent submitted: **1**
- Number of processes with TRL increase: **4**



# WP4 Innovations in metallic treatment and conditioning

## Task4.4: Development and optimization of decontamination processes

---

TOMO SUZUKI-MURESAN & ALL MEMBERS  
OF THE TASK4.4



This project has received funding from the European Union's Horizon 2020 research and innovation programme under grant agreement No 945098.

## Context & Objectives

---

- Multiple origins of metallic wastes
  - Nuclear power plants: maintenance, dismantling, decommissioning
  - Nuclear facilities for retreatment and reprocessing
- Dismantling and decommissioning
  - Very large volumes of waste: Metallic components one of the main contributor of the inventory  
⇒ may over-saturate the capacity of waste disposal repository.
- Typical metals studied in this task include Ni-alloys and stainless steels.
- Objectives:
  - Developing and optimizing decontamination procedure
  - Minimizing secondary effluent wastes



# Approaches & Methodologies

Sample preparation

Treatment of metallic wastes

Secondary waste treatment

Oxidized samples  
representing NPP and  
reprocessing facility



HNO<sub>3</sub> Permanganate Oxalic acid  
(COREMIX)



Preparation of decontamination  
loop by APOX optimization



Vacuumable  
decontamination gels



Electrochemical gel  
decontamination (EASD)

Precipitation  
Electrocoagulation



*Presentation M. Robin*

Ionic Liquid  
decontamination



Electrochemical  
deposition from  
ionic liquids

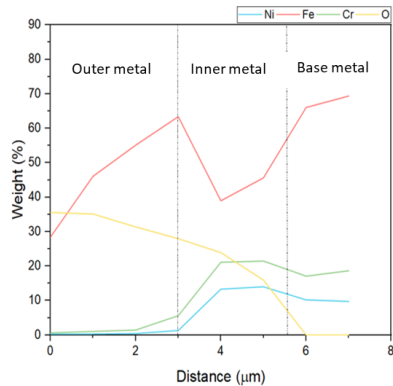
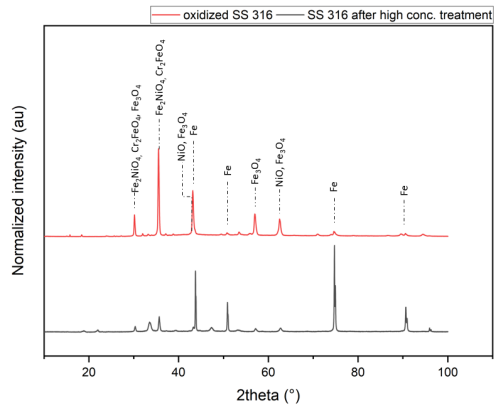


 **Interaction with WP2 LCC/LCA**



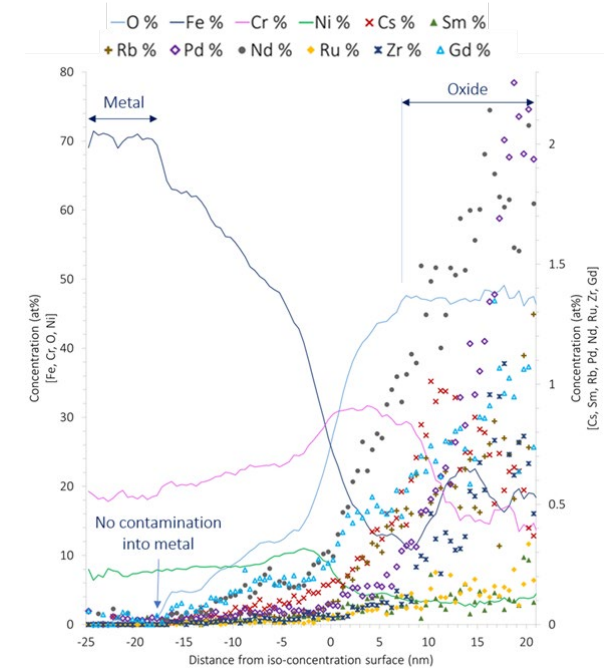
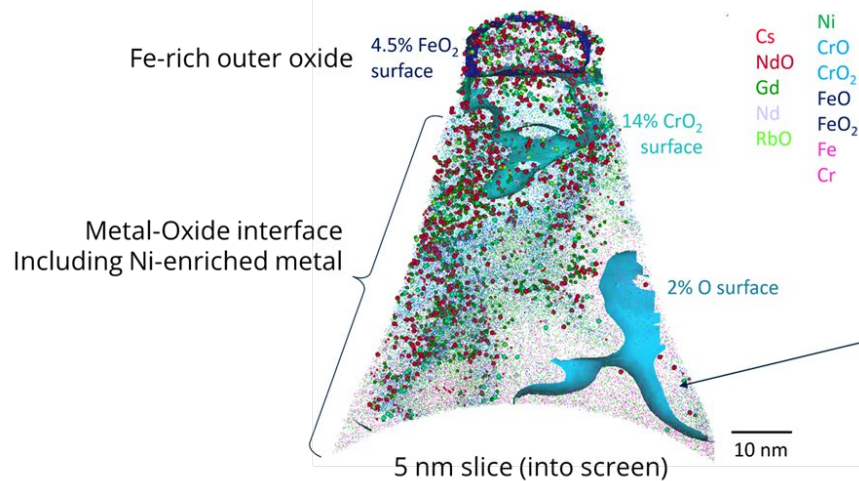
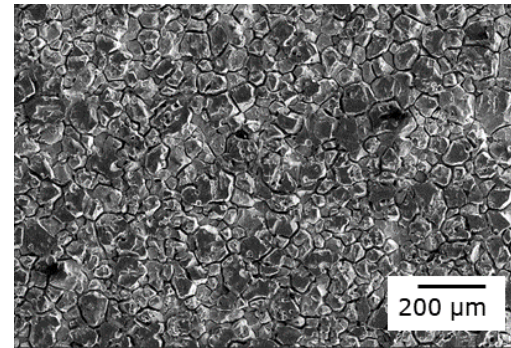
# Sample preparation with contaminants and characterisation

Metal heated up via induction and water vapour is used to form oxide layer



Multilayer oxide representative of the primary circuit and consisting of various oxides of Fe, Ni and Cr.

Successful 3D characterization of the contaminated oxide layer  
Stainless steel boiled in 8M HNO<sub>3</sub> and contaminants

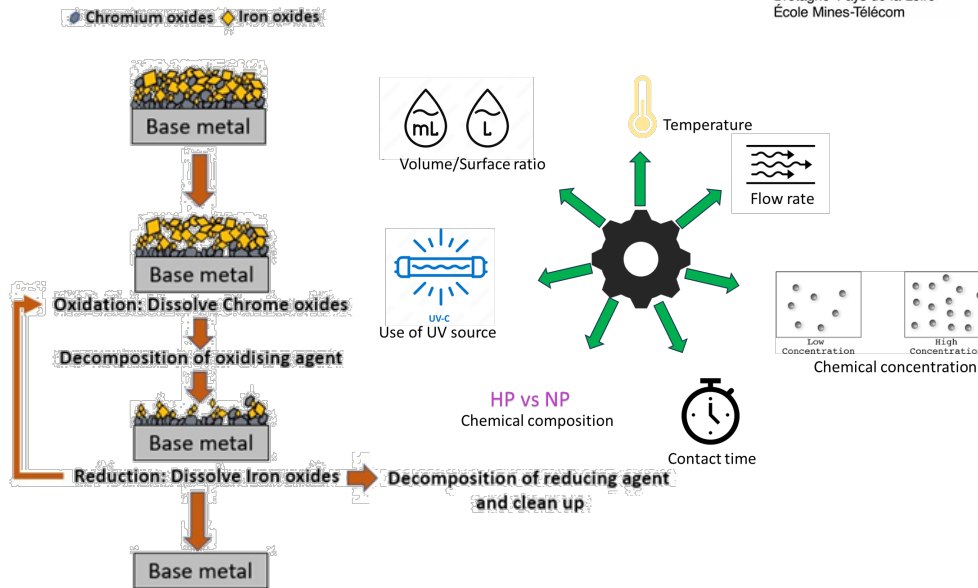
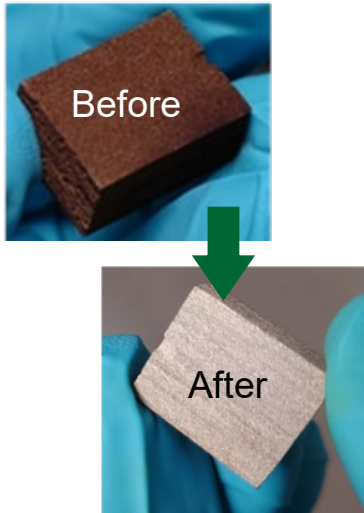


Metal only (tip mostly oxide)



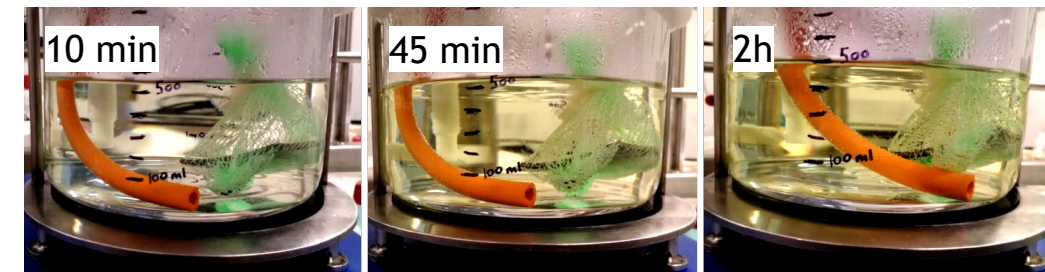
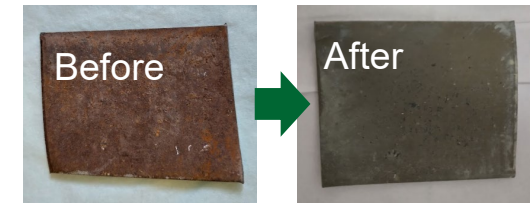
# Optimizing chemical decontamination using Oxidation Reduction Decontamination Process

## COREMIX



## APOX

- Optimizing and upscaling existing process using decontamination loop
- Ready for further testing



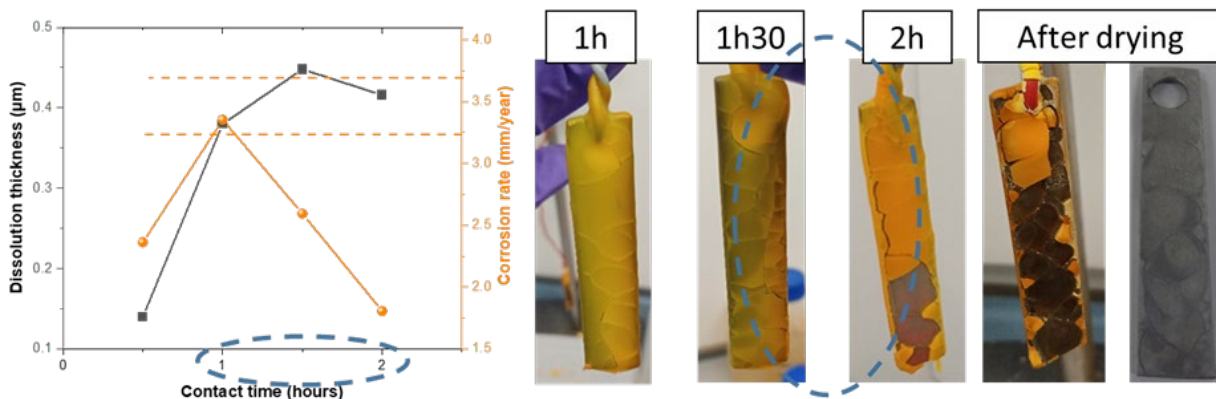
Coloration of the solution during leaching

- Alternating steps of  $\text{HNO}_3/\text{KMnO}_4$  and  $\text{H}_2\text{C}_2\text{O}_4$  → no additional clean-up required
- Process found to be optimal on SS and Ni-alloys from NPPs and reprocessing plants



# Decontamination of metallic waste using inorganic gels

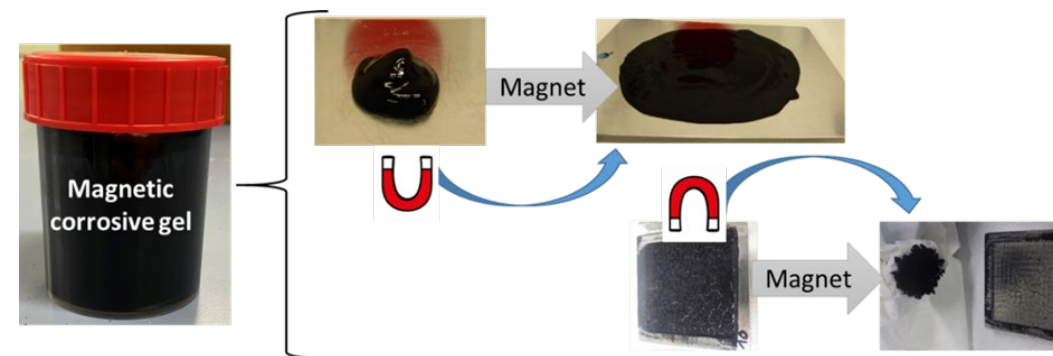
## Model system : Gel HNO<sub>3</sub> + Ce(IV) on non-oxidized SS



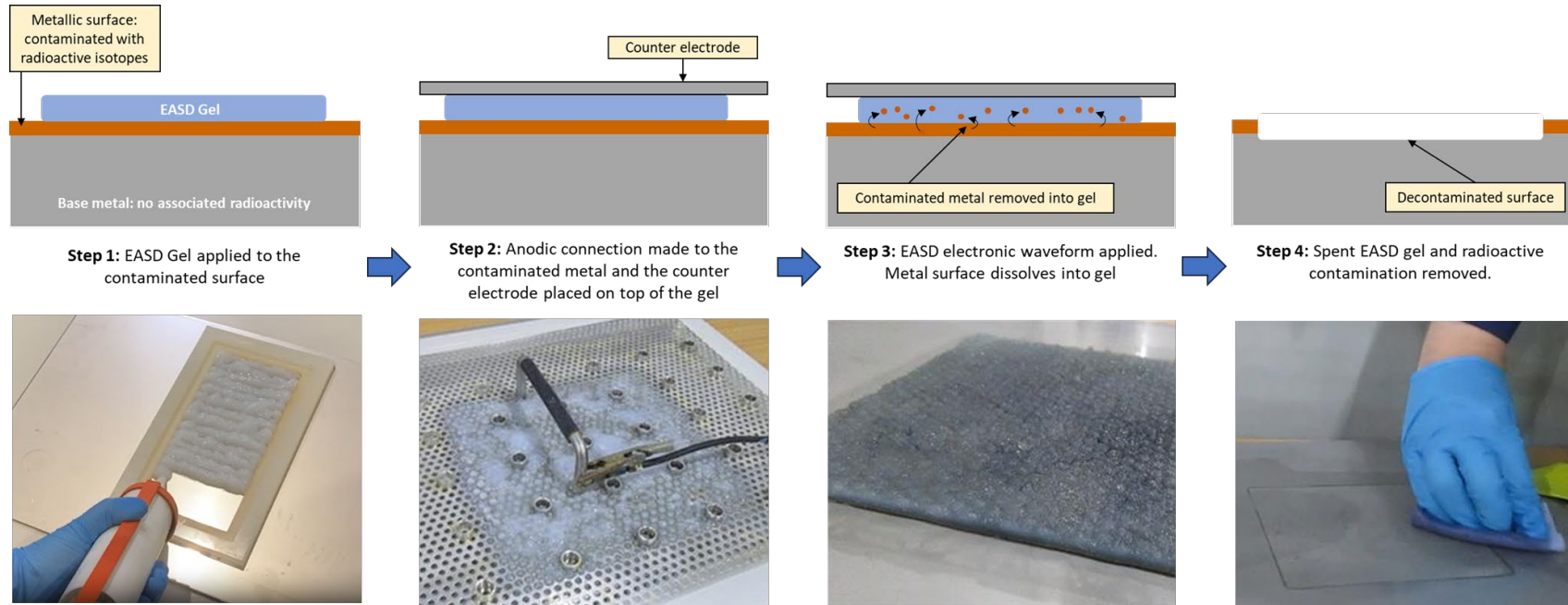
- Adhesion on surfaces without flowing  
→ contact between surface and solution
- Smooth corrosion ( $\approx \mu\text{m}$ ) and absorption of the contamination
- No secondary effluent, only solid waste

New gel formulation integrating magnetic particles to be remotely applied with a magnet (for hardly accessible surfaces)

## New gel formulations based on the COREMIX process



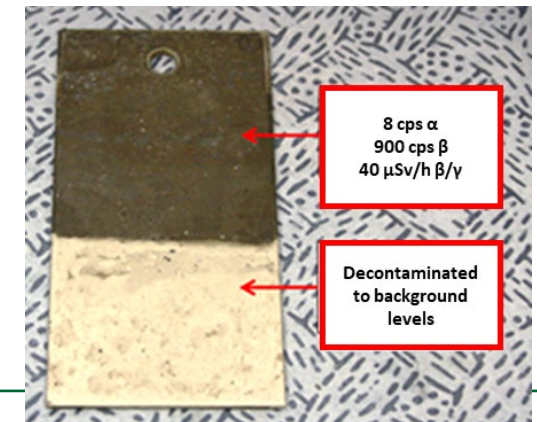
## Electrochemical gel decontamination (EASD)



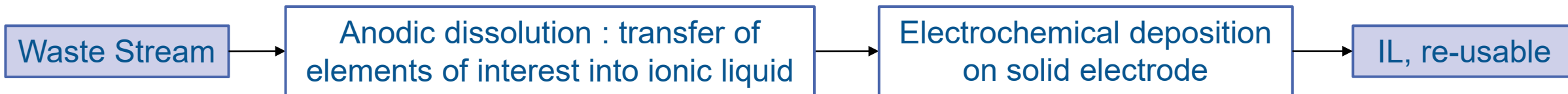
Step-by-step process

### Key Benefits:

- No aggressive chemicals, only electricity
- Simple secondary waste form
- Treatment is fast (~0.5µm/min removal for stainless steel)
- High DF's achievable
- Can be deployed in-situ to target radiation hot spots



# Coupling anodic dissolution and electrodeposition



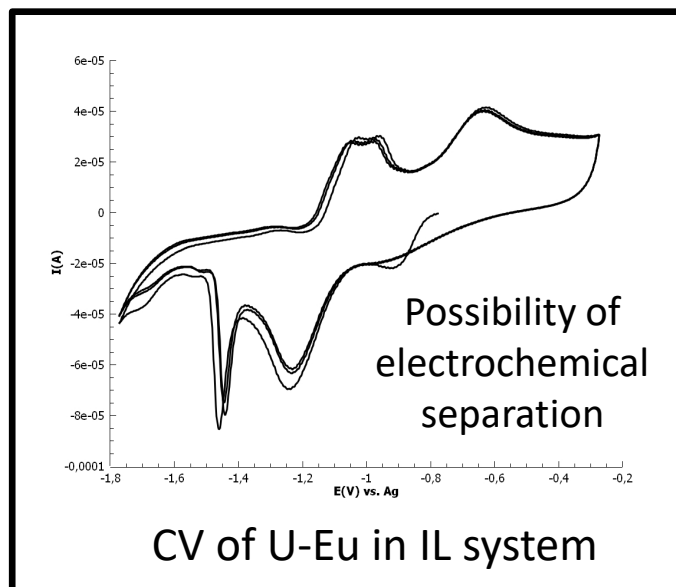
NATIONAL NUCLEAR LABORATORY



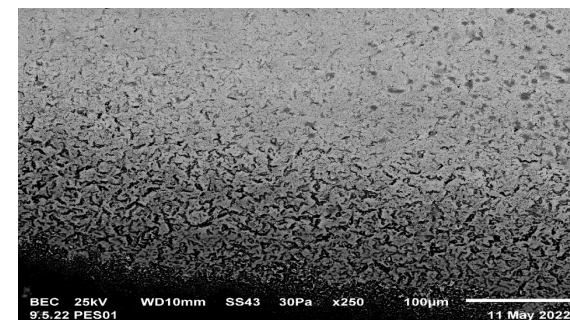
Before



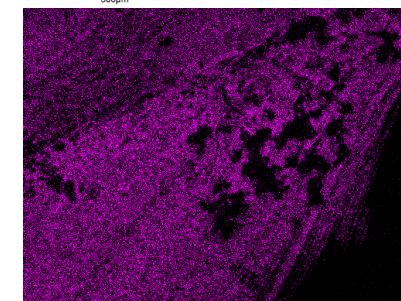
After



Deposited element of interest



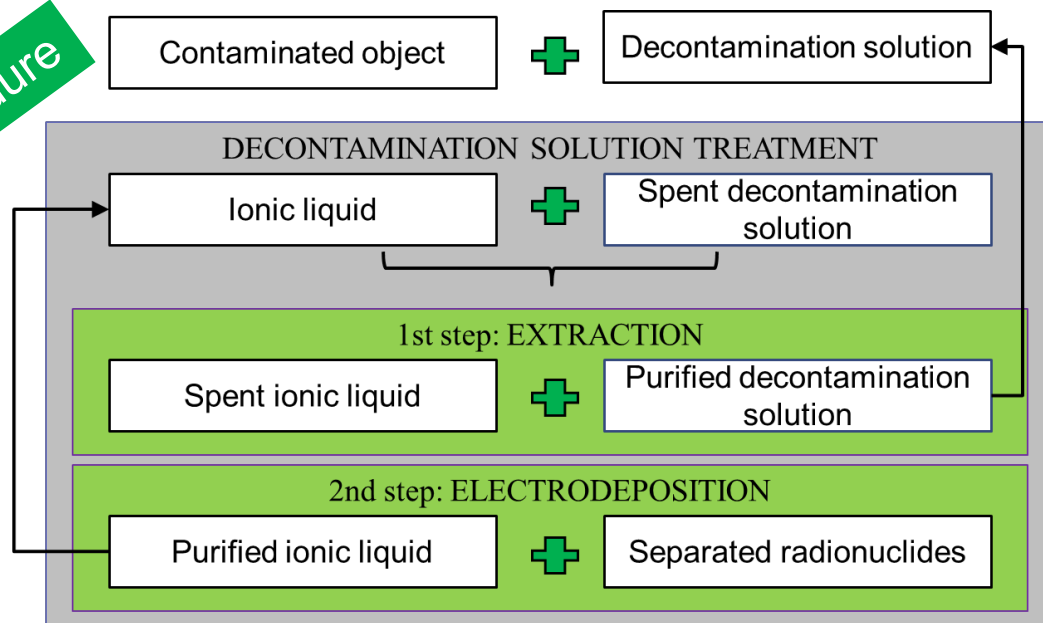
Mixed deposit incl. Nd, Sm, Eu, Gd leading to clean IL



300µm

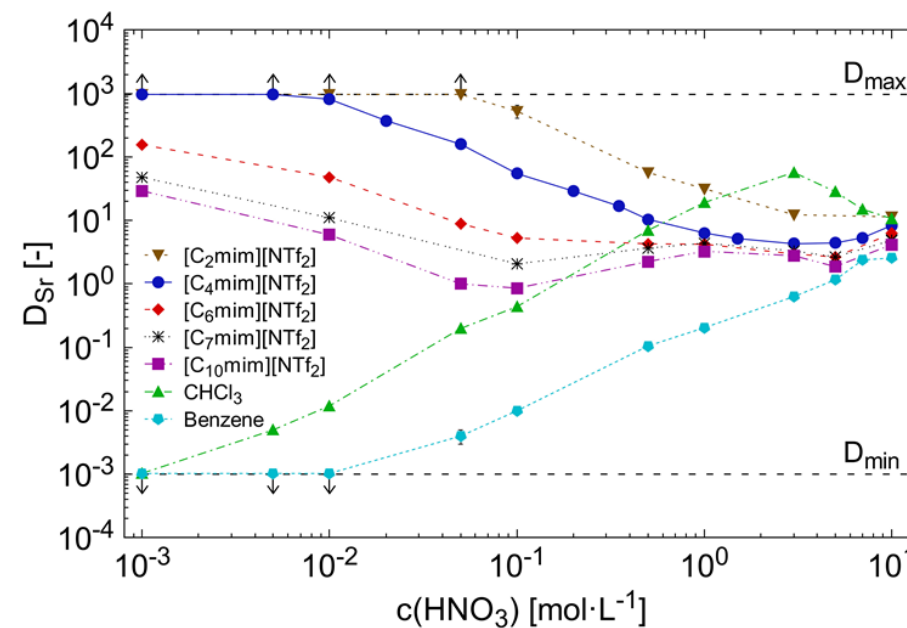
# Coupling liquid/liquid extraction and electrodeposition

procedure



- Extraction of radionuclides from model decontamination solution → Possibility to regenerate solution
- Regeneration of spent ionic liquid by electrochemical treatment.

- Ionic liquid extraction
  - Activation products (Co, Fe)
  - Fission products (Sr, Mo, Tc)



# New Skills and Collaborations



**Training School at La Hague, France**



**NNL, UK**



**IMT Atlantique, France**



**Mobility program**



**PREDIS workshop, Belgium (2023)**



**Guest seminar presentations**



Applied Radiation and Isotopes  
Volume 181, March 2022, 110073  
<https://doi.org/10.1016/j.apradiso.2021.110073>

**Tafel-analysis of the AP-CITROX decontamination technology of Inconel alloy 690**

R. Katona<sup>a</sup>, A. Rivonkar<sup>b</sup>, R. Locskai<sup>a</sup>, G. Bátor<sup>c</sup>, A. Abdelouas<sup>b</sup>, J. Somlai<sup>c</sup>, T. Kovács<sup>a,c</sup>  

Progress in Nuclear Energy  
Volume 149, July 2022, 104255  
<https://doi.org/10.1016/j.pnucene.2022.104255>

Review

**Gels, coatings and foams for radioactive surface decontamination: State of the art and challenges for the nuclear industry**

Alban Gossard<sup>a</sup>  , Audrey Lilin<sup>b</sup>, Sylvain Faure<sup>a</sup>

**Optimisation of the chemical oxidation reduction process (CORD) on surrogate stainless steel in regards to its efficiency and secondary wastes** <https://doi.org/10.3389/fnuen.2022.1080954>

 Aditya Rivonkar<sup>1\*</sup>  Richárd Katona<sup>2,3</sup>  Mathurin Robin<sup>1</sup>  Tomo Suzuki-Muresan<sup>1</sup>

 Abdessalam Abdelouas<sup>1</sup>  Marcel Mokili<sup>2</sup>  Gergő Bátor<sup>2,3</sup>  Tibor Kovács<sup>2,3</sup>

Journal of Radioanalytical and Nuclear Chemistry  
<https://doi.org/10.1007/s10967-023-09293-6>

<https://link.springer.com/article/10.1007/s10967-023-09293-6>

**Liquid-liquid extraction of strontium from acidic solutions into ionic liquids using crown ethers**

Jan Houzar<sup>1</sup>  · Katerina Cubova<sup>1</sup> · Miroslava Semelova<sup>1</sup> · Mojmir Nemeč<sup>1</sup>

Progress in Nuclear Energy  
Volume 159, May 2023, 104637  
<https://doi.org/10.1016/j.pnucene.2023.104637>

Review

**A review of contamination of metallic surfaces within aqueous nuclear waste streams**

Daniel N.T. Barton<sup>a</sup>  , Thomas Johnson<sup>a</sup>, Anne Callow<sup>b</sup>, Thomas Carey<sup>b</sup>, Sarah E. Bibby<sup>c</sup>, Simon Watson<sup>a</sup>, Dirk L. Engelberg<sup>d</sup>, Clint A. Sharrad<sup>a</sup>

Environmental Technology & Innovation  
Volume 35, August 2024, 103688  
<https://doi.org/10.1016/j.eti.2024.103688>

**Colloidal magnetic gels for the decontamination of limited access metallic surfaces**

Hippolyte Pochat-Cottilloux<sup>a</sup>, Fabien Frances<sup>a</sup>, Luc Girard<sup>b</sup>, Aditya Rivonkar<sup>c</sup>, Alban Gossard<sup>a</sup>  

**Methods for the destruction of oxalic acid decontamination effluents**

 Jessica Blenkinsop<sup>1\*</sup>  Aditya Rivonkar<sup>2</sup>  Mathurin Robin<sup>2</sup>  Thomas Carey<sup>1</sup>

 Barbara Dunnett<sup>1</sup>  Tomo Suzuki-Muresan<sup>2</sup>  Cavit Percin<sup>2</sup>  Abdessalam Abdelouas<sup>2</sup>  Jonathan Street<sup>3</sup> <https://doi.org/10.3389/fnuen.2024.1347322>

**Optimized precipitation process for the treatment of radioactive effluents from Ni-alloy decontamination using a Chemical Oxidation Reduction process** Provisionally Accepted

<https://doi.org/10.3389/fnuen.2024.1396821>

 Mathurin Robin<sup>1\*</sup>  Aditya Rivonkar<sup>1</sup>  Tomo Suzuki-Muresan<sup>1</sup>

Abdessalam Abdelouas<sup>1</sup> Marcel Mokili<sup>2</sup>

**Caesium and strontium contamination on NAG 18/10L stainless steel following corrosion in simulated nitric acid reprocessing liquor**

Anne Callow<sup>1,2\*</sup>, Dean Connor<sup>1,3</sup>, Thomas Carey<sup>1,4</sup>, Kim Summers<sup>1</sup>, Christina Hofer<sup>2</sup>, Kerstin Jurkschat<sup>2</sup>, Jonathan Street<sup>5</sup>, Sarah Bibby<sup>5</sup>

<sup>1</sup> National Nuclear Laboratory, Central Laboratory, Sellafield, Seascale, Cumbria, CA20 1PG, UK

<sup>2</sup> Department of Materials, University of Oxford, Parks Road, Oxford, OX1 3PH, UK

<sup>3</sup> Interface Analysis Centre, School of Physics, University of Bristol, HH Wills Physics Laboratory, Queens Rd, Bristol BS8 1QU, UK

<sup>4</sup> University of Birmingham, Edgbaston, Birmingham, B15 2TT, UK

<sup>5</sup> Sellafield Ltd., Seascale, Cumbria, CA20 1PG, UK

\* Email: anne.callow@uknnl.com

Manuscript currently under review, Corrosion Science



This project has received funding from the Euratom research and training programme 2019-2020 under grant agreement No 945098.

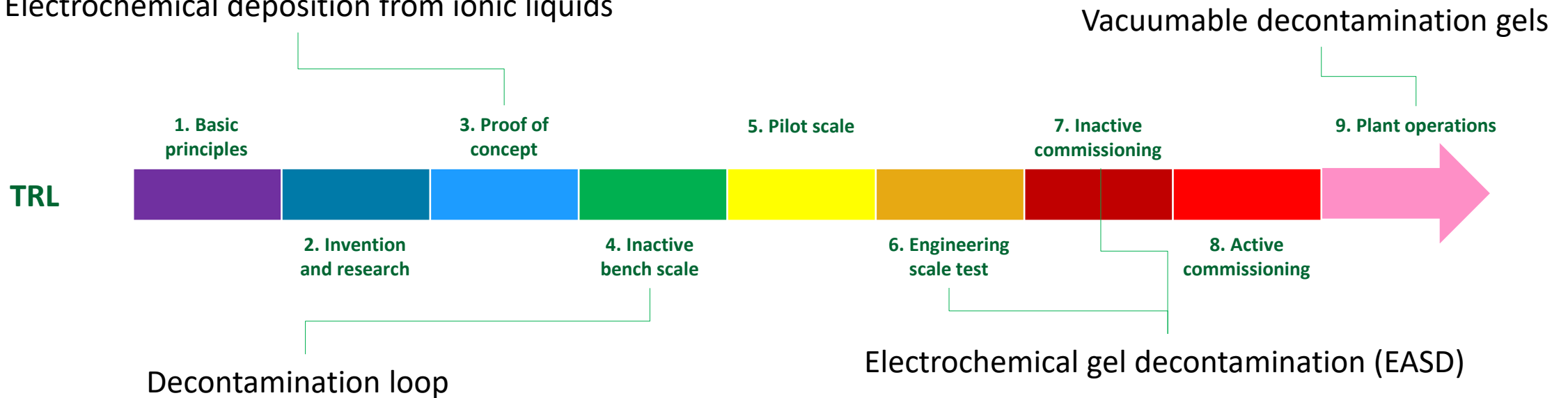
## Achievements and Perspectives

- HNO<sub>3</sub> Permanganate Oxalic acid (COREMIX)
- Precipitation, Electrocoagulation
- Magnetic and COREMIX decontamination gels
- Electrochemical deposition from ionic liquids

⇒ Upscaling liquid effluent treatment  
 ⇒ Upscaling magnetic gel technology  
 ⇒ Innovation for matrix conditioning

Contributions in EURAD2

- WP STREAM
- WP LOPERA





# Contributions

---



Alban Gossard, Fabien Frances, Hippolyte Pochat-Cottilloux, Gabriella Lucena



Kateřina Čubová, Mojmir Nemeč



Aditya Rivonkar, Mathurin Robin, Abdesselam Abdelouas, Marcel Mokili



Thomas Carey, Anne Callow, Jess Blenkinsop, Rhianna Jobson, Moya Hay



Richard Katona, Gergő Bátor, Tibor Kovács



Martin Straka

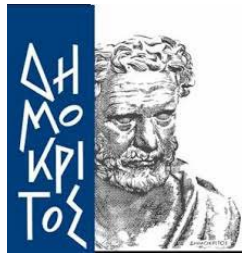


This project has received funding from the Euratom research and training programme 2019-2020 under grant agreement No 945098.



# PREDIS

## **T4.5 Optimization of characterization techniques and waste minimization**



A. Savidou, NCSR

# Participants

M. C. BORNHOEFT  
DMT

[MarieCharlotte.Bornhoeft@dmt-group.com](mailto:MarieCharlotte.Bornhoeft@dmt-group.com)

F. GAGLIARDI  
NUCLECO

[Gagliardi@nucleco.it](mailto:Gagliardi@nucleco.it)

E. LAGZDINA  
FTMC

[elena.lagzdina@ftmc.lt](mailto:elena.lagzdina@ftmc.lt)

A. MARKOPOULOS  
NCSR

[angelos@ipta.demokritos.gr](mailto:angelos@ipta.demokritos.gr)

RITA PLUKIENE  
FTMC

[rita.plukiene@ftmc.lt](mailto:rita.plukiene@ftmc.lt)

E. LANGEGER  
DMT

[Eileen.Langegger@dmt-group.com](mailto:Eileen.Langegger@dmt-group.com)

F. GENTILE  
NUCLECO

[Gentile@nucleco.it](mailto:Gentile@nucleco.it)

J. L. LEGANES NIETO  
ENRESA

[jlen@enresa.es](mailto:jlen@enresa.es)

D. MAVRIKIS  
NCSR

[d.mavrikis@ipta.demokritos.gr](mailto:d.mavrikis@ipta.demokritos.gr)

A. SAVIDOU  
NCSR

[savidou@ipta.demokritos.gr](mailto:savidou@ipta.demokritos.gr)

St.. CONINX & J. FEINHALS  
Former DMT

D. E. HERNANDO  
ENRESA

[DESH@enresa.es](mailto:DESH@enresa.es)

A. LESKINEN  
VTT

[Anumaija.Leskinen@vtt.fi](mailto:Anumaija.Leskinen@vtt.fi)

M. NEMEC  
CTU

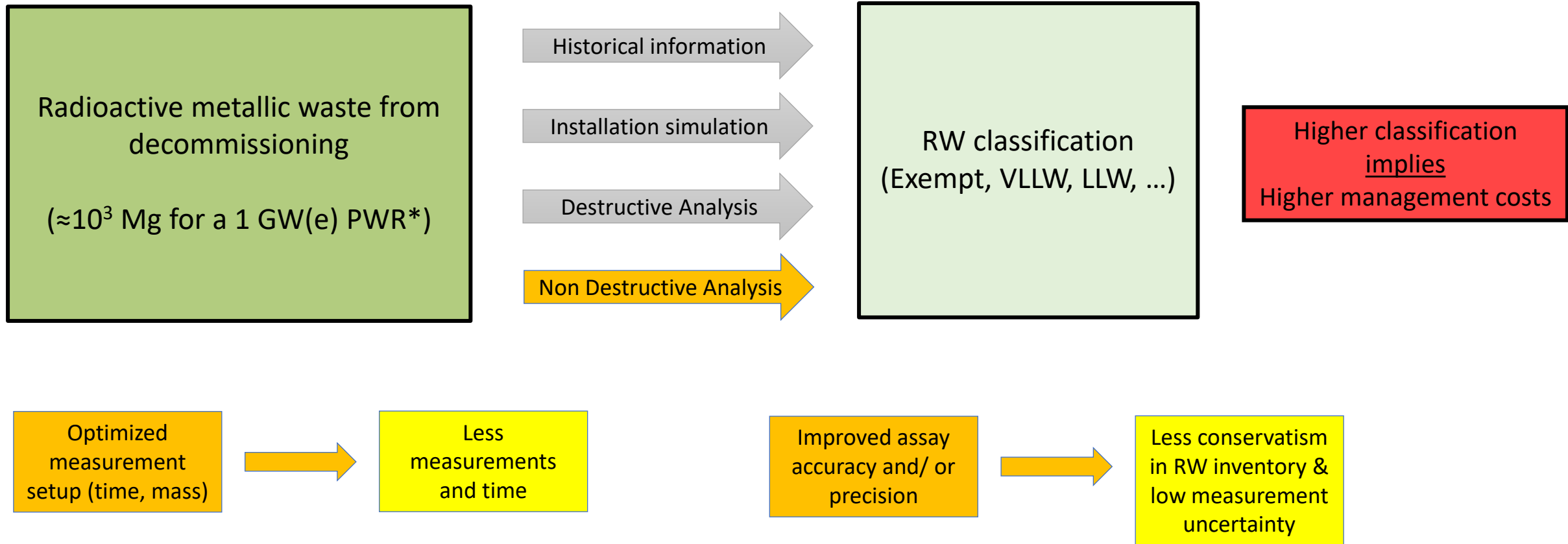
[mojmir.nemec@fifi.cvut.cz](mailto:mojmir.nemec@fifi.cvut.cz)

T. SUZUKI-MURESAN  
IMT

[suzuki@subatech.in2p3.fr](mailto:suzuki@subatech.in2p3.fr)



# *Necessity for optimization of metallic waste characterization & procedures for minimization and recycling*



\*IAEA, TECHNICAL REPORTS SERIES No. 401

# Metallic waste management routes

Mech./ chem. decontamination & clearance



Reuse & Recycling

Reuse for other purpose



Recycling

Shielding



Cask Production



Inside the control area

Disposal as radioactive waste

# Classification of the waste streams (1)

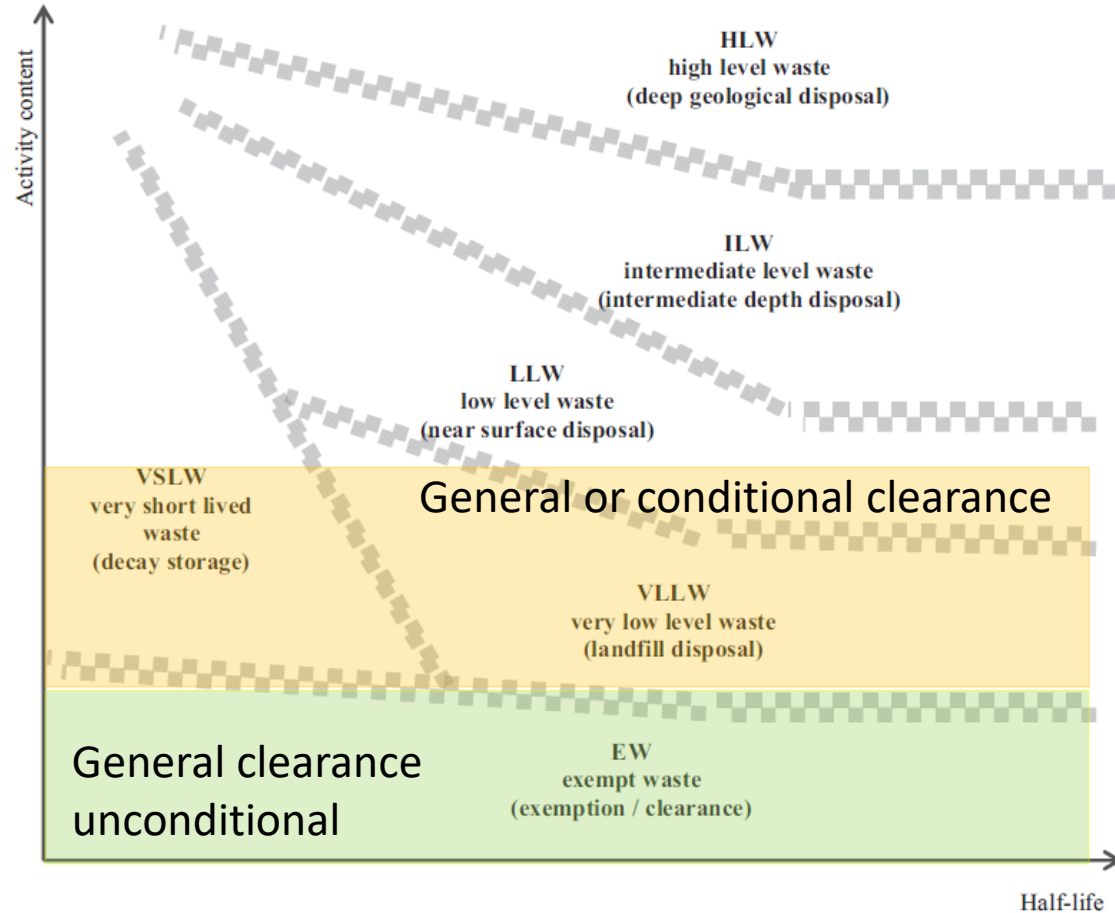


FIG. 1. Conceptual illustration of the waste classification scheme. (according to IAEA)

**CLASSIFICATION:** Quantification of specified radionuclides to comply with management route requirements or disposal site performance objectives.

**The aim of classification of the metallic radioactive waste is changing together with the activity:**

- **HLW & ILW** for radiation protection and best packaging concept
- **LLW** to demonstrate compliance with the WAC for engineered near surface facilities or near surface landfill
- **VLLW** to demonstrate compliance with the WAC for near surface landfill or to decide decontamination & clearance/ declassification



**Optimization of sorting**

(The largest volumes of waste from the dismantling of nuclear installations are EW, VLLW and LLW)

# Classification of the waste streams (2)

## Similar for all nuclear reactors:

- Reactor operation generates fission, activation & corrosion products
- ETM & DTM radionuclides
- Methodology for classification of reactor components (neutron calculations, scaling factors)
- Scaling factors and Nuclide Vector methodology

## Different for nuclear reactors:

- Composition of different nuclear reactors metallic components
- Neutron energy distribution & fluence
- Time after reactor shutdown
- Extent & activity of long-lived neutron activation products
- Extent & activity of neutron activated, fission & corrosion products released to reactor coolant

VOLUME AND ACTIVITY OF LILW GENERATED ANNUALLY BY  
1 GWe NUCLEAR POWER PLANT (according to IAEA-TECDOC-1591)

Reactor type	Volume (m <sup>3</sup> )	Activity (TBq)
ABWR	500*	500*
AGR	650	600*
BWR	500	500
FBR	500*	500*
GCR	5000	1000*
LWGR (RBMK)	1500	1000*
PHWR	200	100*
PWR	250	100
WWER	600	600

\* Values marked with an asterisk, were not taken from references, and are estimates, pending the availability of reliable information.

Pre-dismantling classification using a modeling approach & the scaling factors methodology allows sorting of metallic waste with regard to the level of activity and radionuclides presented in **waste streams**

# Scaling Factors (1)

## Finding correlation between Difficult to Measure isotopes, DTM, and Easy to Measure, ETM (Key Nuclides)

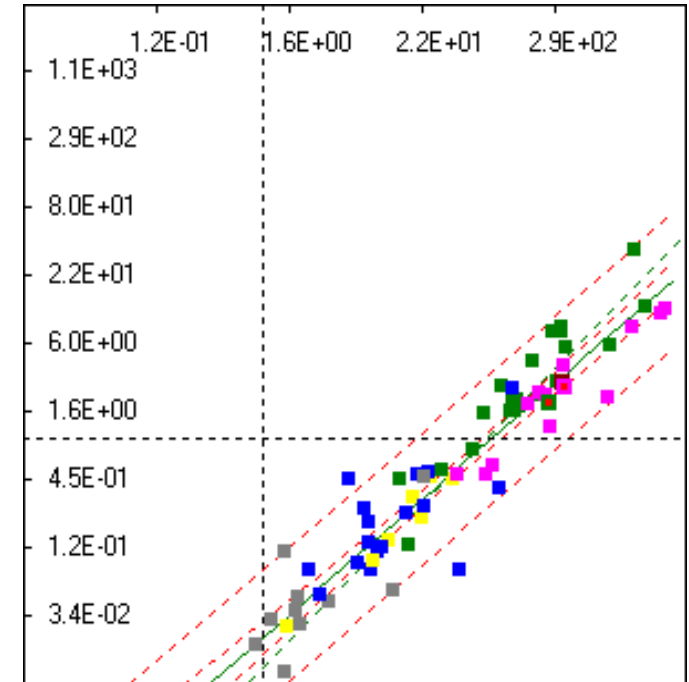
### Key Nuclides (K.N.):

- Gamma emitter easily detected for any gamma spectrometry
- Relatively long lived ( $^{60}\text{Co}$  and  $^{137}\text{Cs}$ )

### Difficult to Measure Isotopes and K.N.:

- Activation Products (AP), or Fission Products (FP)
- Similar solubility
- Similar transport process

- 1) ISO 21238 “Scaling factor method to determine the radioactivity of low and intermediate-level radioactive waste packages generated at nuclear power plants”
- 2) IAEA TECDOC NW-T-1.18 “Determination and Use of Scaling Factors for Waste Characterization in Nuclear Power Plants”



- Geometric Mean, Arithmetic Mean, Log-Linear Regression
- Collection of samples, time Consuming, High budget
- Manner of sampling as critical aspect

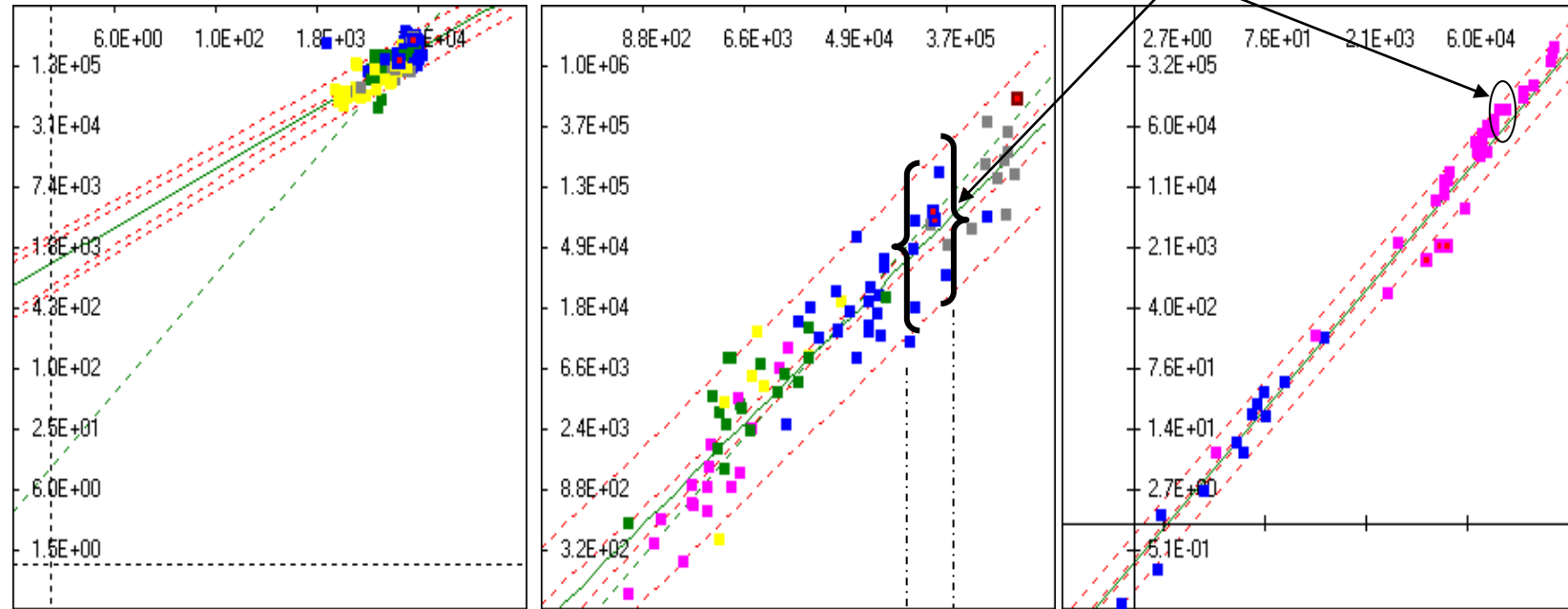
# Scaling Factors (2)

CHARACTERIZATION DESIGN PLANNED IN ORDER TO OBTAIN REPRESENTATIVE SCALING FACTORS

Intermediate Level Waste (ILW)  
 Low Level Waste (LLW)  
 Very Low Level Waste (VLLW)  
 Clearance purposes

REPRESENTATIVENESS OF SCALING FACTORS

Composite samples. Lower number of samples for radiochemical analyses



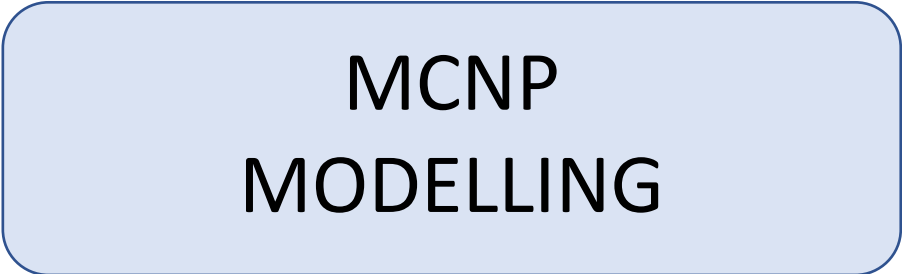
Increasing accuracy

Decreasing uncertainty

**Possibilities of surface and volume activity determination in metallic waste  
by using experimental & MCNP modelling of  $\gamma$ -spectra**

# Innovative Technique for metals characterization – Materials & Methods

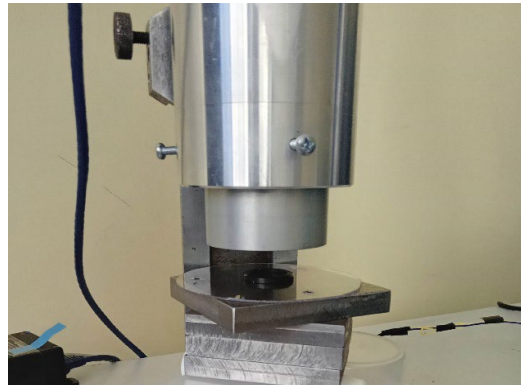
A non-destructive  $\gamma$ -spectrometry technique for interpretation of  $\gamma$ -ray spectra of activated and/or contaminated components.



Experimental spectra have been compared to the modelled ones



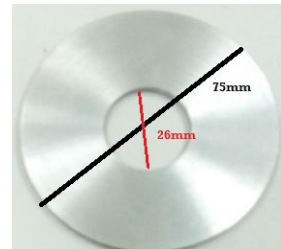
*HPGe spectrometer  
with Pb and steel based  
protection shield*



*CeBr<sub>3</sub> spectrometer  
with metal plates and point source*



*The point source placed  
between two metal plates  
in the hole of Al disk.*



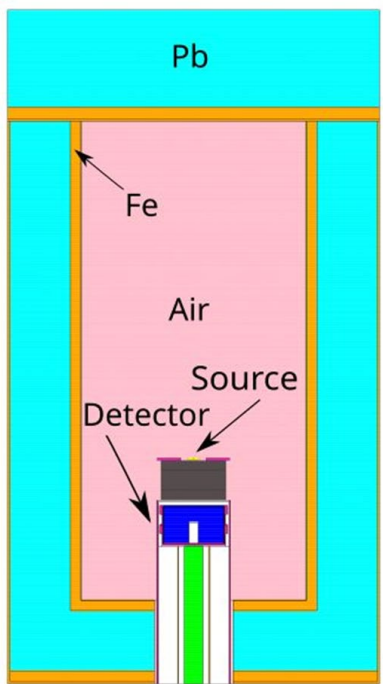
*Dimensions of Al disk*

The activity of point sources:

<sup>137</sup>Cs (60.4±2.0) kBq

<sup>60</sup>Co (1.02±0.03) kBq

# MCNP modelling of $\gamma$ -ray spectra of metallic model samples measured by HPGe detector



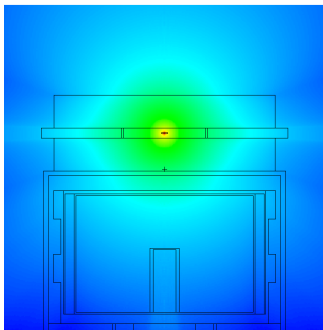
Modelled HPGe detector and  $^{137}\text{Cs}$  photon flux for different geometry "metallic model samples":

(a) HPGe and point source between metal plates in the Al disk (as shown in previous slide),

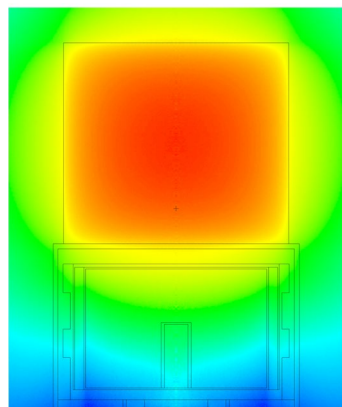
(b) HPGe and volume source,

(c) HPGe planar sources (top picture) 2 cm depth and 4 cm depth (bottom picture) in the metal sample

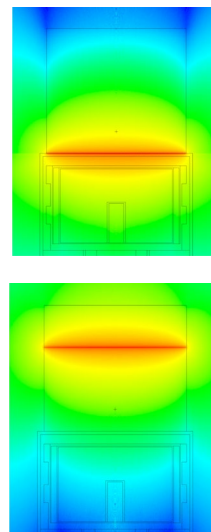
HPGe



a)

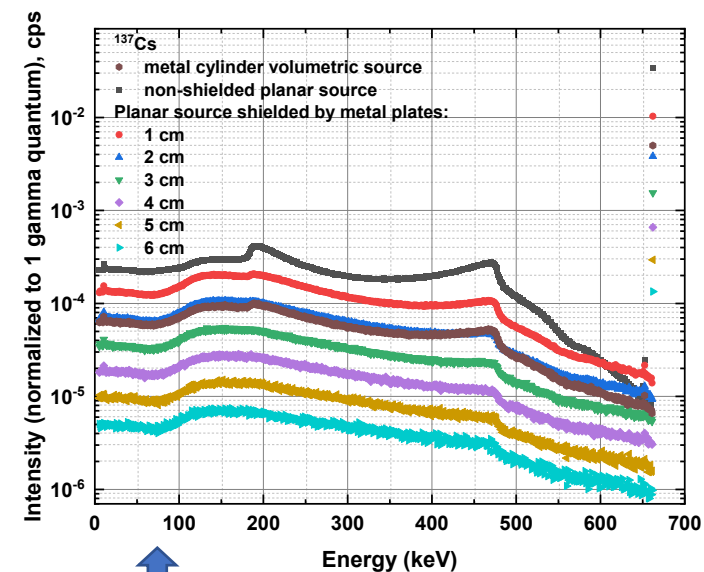


b)



c)

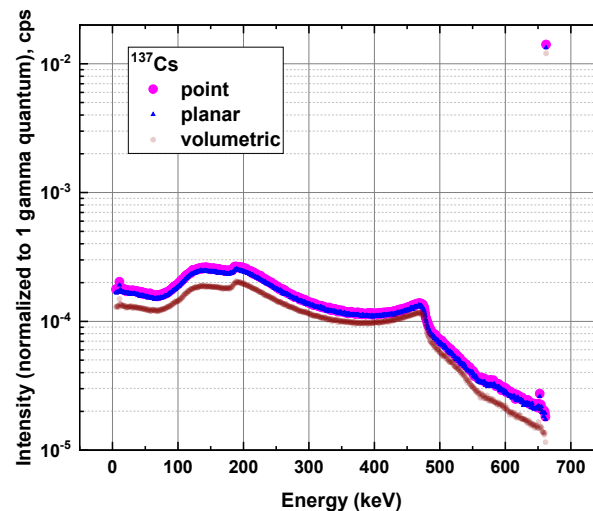
## Comparison of modelled $^{137}\text{Cs}$ $\gamma$ -spectra in HPGe for different source cases



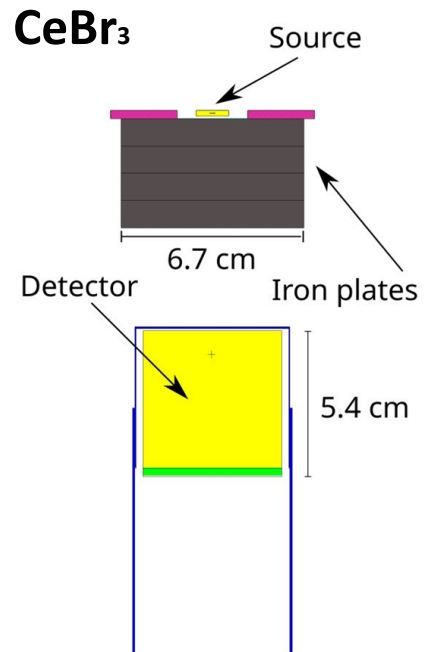
Extended volume sample (distributed homogeneously in the  $h=6\text{ cm}$   $r=3.36\text{ cm}$  metal cylinder) and planar sample shielded with metal plates of different thickness (1-6cm)

Taking into account both *intensity of the photopeak* and *Compton backscatter / peak ratio* of  $\gamma$ -spectra one could separate different shielding or volumetric samples

Point and planar sources shielded by 2 cm metal plate and volumetric source for comparison.



# MCNP modelling of $\gamma$ -ray spectra of metallic model samples measured by $\text{CeBr}_3$ detector

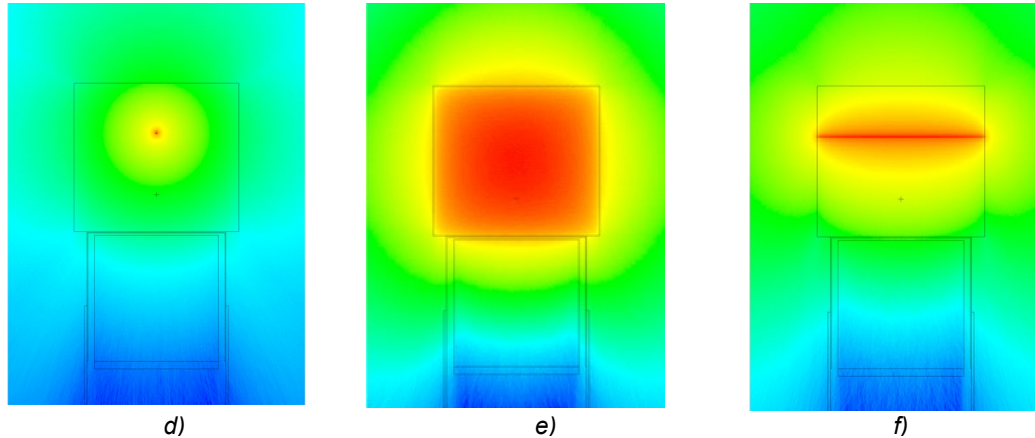


Modelled  $\text{CeBr}_3$  detector and  $^{137}\text{Cs}$  photon flux for different geometry “metallic model samples”:

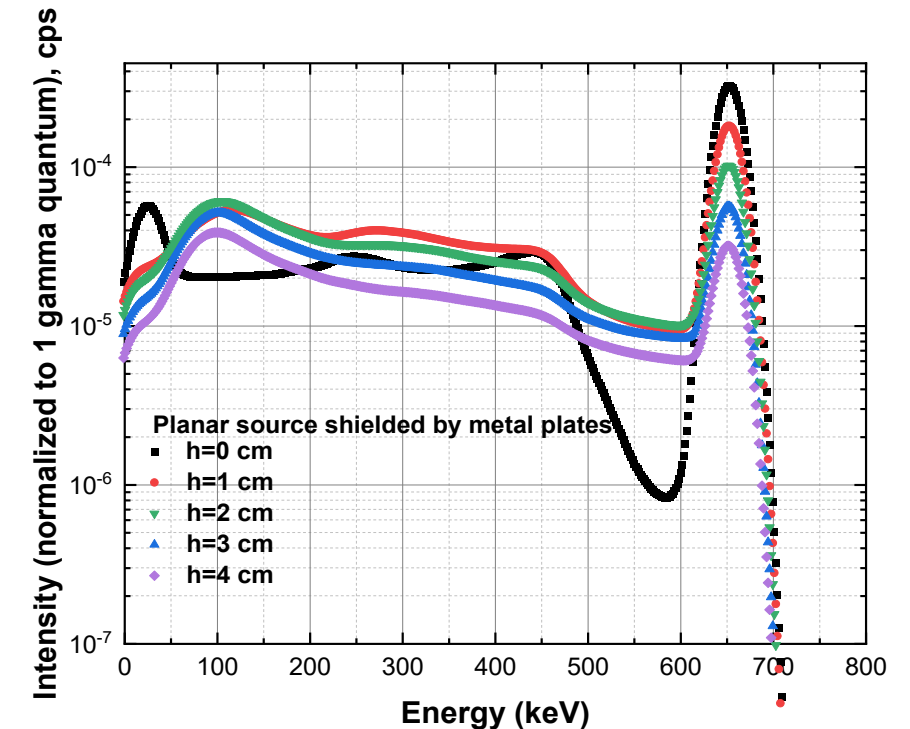
(d)  $\text{CeBr}_3$  detector and point source at 4 cm depth in the metal sample,

(e)  $\text{CeBr}_3$  detector and volume source

(f)  $\text{CeBr}_3$  detector and planar source at 4 cm depth in the metal sample (stack of metal plates)



Modelled  $^{137}\text{Cs}$   $\gamma$ -spectra in  $\text{CeBr}_3$  detector for planar source shielded with metal plates of different thickness.

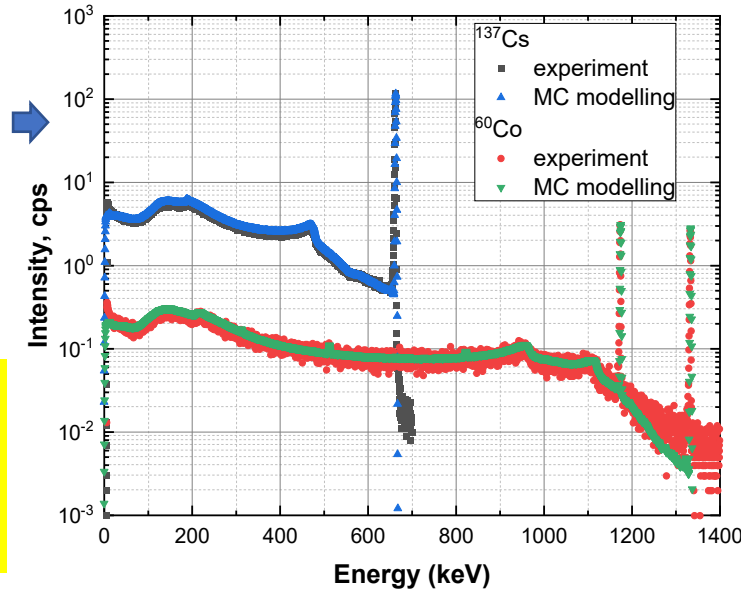


Taking into account both *intensity of the photopeak* and *Compton backscatter /peak ratio* of  $\gamma$ -spectra measured by  $\text{CeBr}_3$  one could separate different shielded planar, point or volumetric sources

# Validation of surface/ volume activity determination in metallic waste samples by using HPGe and CeBr<sub>3</sub> detectors and MCNP modelling of $\gamma$ -ray spectra

## HPGe

A comparison of acquired by the HPGe detector and modelled with MCNP  $\gamma$ -spectra of  $^{60}\text{Co}$  and  $^{137}\text{Cs}$  point sources shielded by 1cm thickness iron plates.



The agreement of HPGe  $\gamma$ -spectra experimental and modelled results is good for different  $^{60}\text{Co}$  and  $^{137}\text{Cs}$  point sources cases

Comparison of simulated and experimental Compton (backscatter)- to-Peak ratios of  $^{137}\text{Cs}$  and  $^{60}\text{Co}$  point sources obtained with HPGe detector.

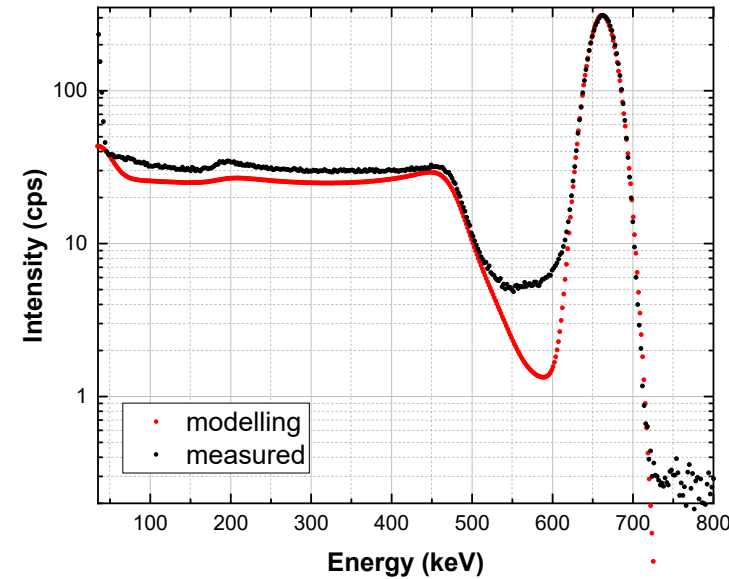
Thickness, cm	Modelled $^{137}\text{Cs}$ (661.6 keV)	Experimental $^{137}\text{Cs}$ (661.6 keV)	Modelled $^{60}\text{Co}$ (1173.2 keV)	Experimental $^{60}\text{Co}$ (1173.2 keV)
0	0.021±0.001	0.018±0.002	0.033±0.005	0.03±0.01
1	0.054±0.003	0.042±0.005	0.09±0.01	0.09±0.03
2	0.091±0.007	0.07±0.02	0.15±0.02	0.16±0.08
3	0.13±0.01	0.10±0.02	0.21±0.03	0.22±0.15
4	0.19±0.02	0.17±0.04	0.28±0.04	0.29±0.15

Comparison of simulated and experimental Compton (backscatter)- to-Peak ratios of  $^{137}\text{Cs}$  point source obtained with CeBr<sub>3</sub> detector.

\* experiment in the open air/ no laboratory environment

## CeBr<sub>3</sub>

Thickness, cm	Modelled $^{137}\text{Cs}$ (661.6 keV)	Experimental $^{137}\text{Cs}$ (661.6 keV)
0*	0.20±0.01	0.19±0.02
0	0.5±0.2	0.5±0.04
1	0.7±0.2	0.9±0.1
2	0.9±0.2	1.3±0.2
3	1.1±0.3	1.8±0.3
4	1.2±0.4	2.4±0.4

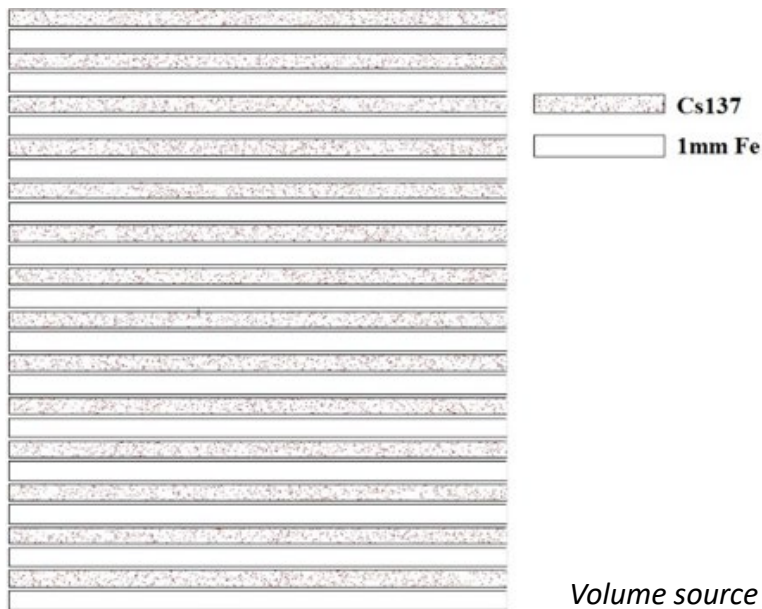


Inter-comparison of  $\gamma$ -spectra of  $^{137}\text{Cs}$  acquired by the CeBr<sub>3</sub> detector and modelled in case of point source on the surface of metal plate (no laboratory environment).

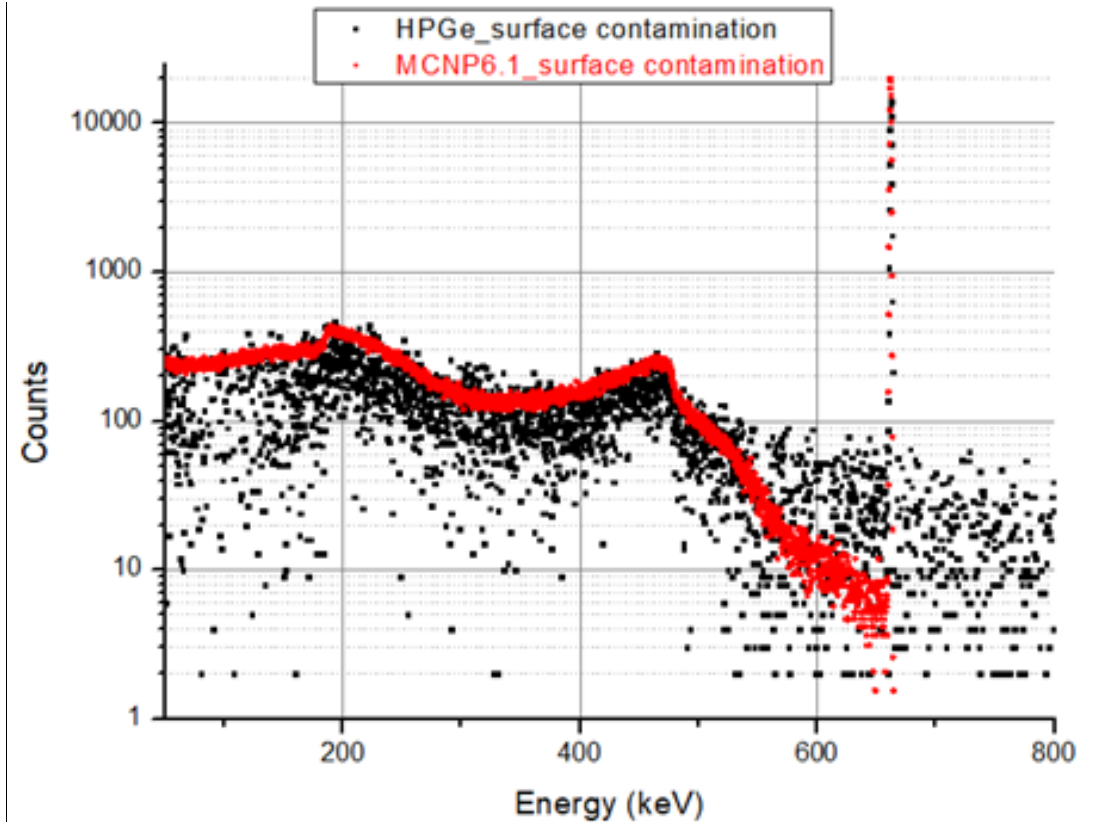
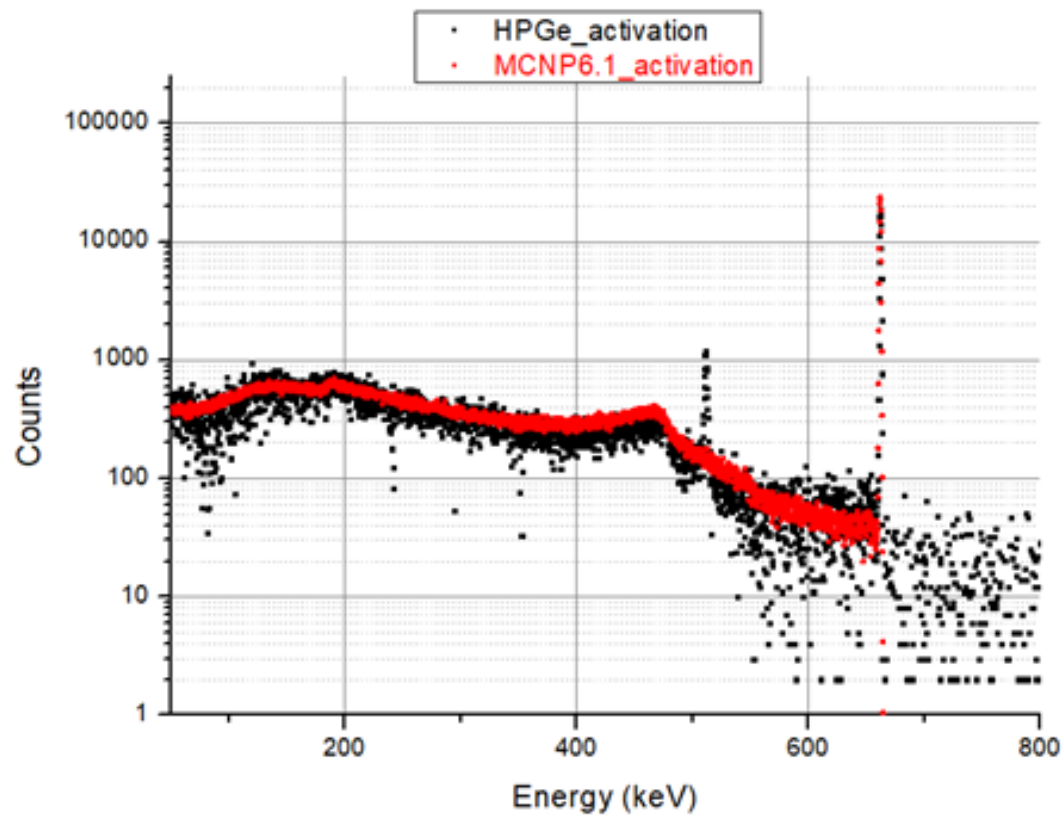
The agreement of experimental and modelled results for  $^{137}\text{Cs}$  point source C/P ratio obtained with CeBr<sub>3</sub> detector is not very good because of not enough accurate modelling of laboratory environment (shielding thickness h=0 cm to h=4 cm cases). Environments significantly influences shape of Compton region.

# Determination of activities on the surface and in the volume

- Volume source representing the activated metallic slab with  $^{137}\text{Cs}$  (instead of  $^{60}\text{Co}$ ) as well as the contamination on the surface with  $^{137}\text{Cs}$  were prepared at the Radioactive Waste and Material Laboratory in the NCSR D.
- Filter paper was subdivided into squares of  $9\text{ cm}^2$  each and  $0.05\text{ ml}$  of  $^{137}\text{Cs}$  acid solution ( $2\text{ M HNO}_3$ ) of  $170 \pm 17\text{ Bq/ml}$  in the centre of each square. The total surface of the contaminated with  $^{137}\text{Cs}$  filter paper was  $5940\text{ cm}^2$ . The total surface was subdivided into 18 sheets of  $33 \times 10\text{ cm}^2$ . Hence, the activity for each one of the 18 contaminated sheets was  $304 \pm 30\text{ Bq}$ . ( $0.92\text{ Bq/cm}^2$ )



*Volume source representing the activated slab for validation of MCNP6.1 models (VisedX\_24E)*



Comparing simulated and real spectra of volume sources representing a) the activated ( $^{137}\text{Cs}$  was used instead of  $^{60}\text{Co}$ ) and b) contaminated metallic slab

# Distinguishing activation and surface contamination (HPGe)

*#Counts of the photopeak for activated slab with surface contamination =  $\lambda_1 \times A(b) + \lambda'_1 \times A'(b)$*

*#Counts of the Compton edge for activated slab with surface contamination =  $\lambda_2 \times A(b) + \lambda'_2 \times A'(b)$*

Where:

$$\lambda_1 = \frac{\text{\# Counts of the photopeak in the activated metallic slab}}{A(a)}$$

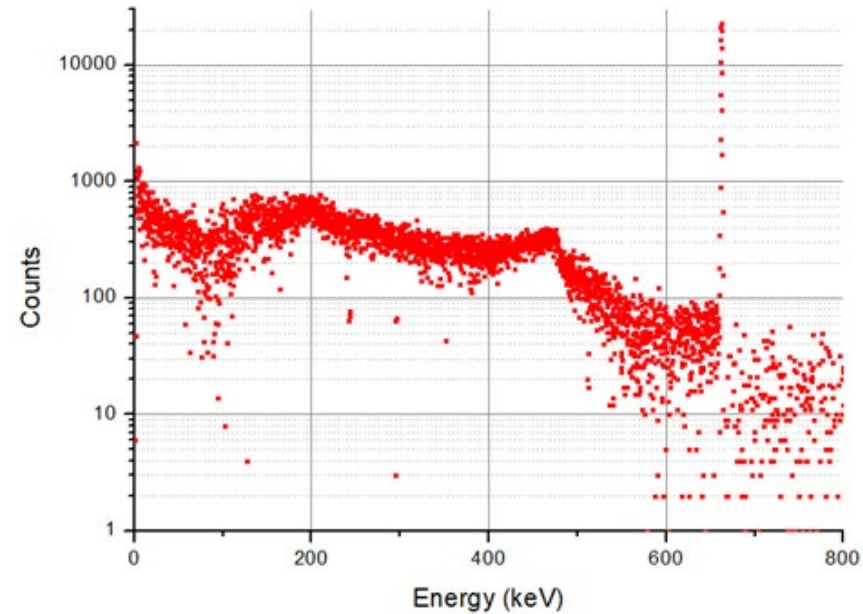
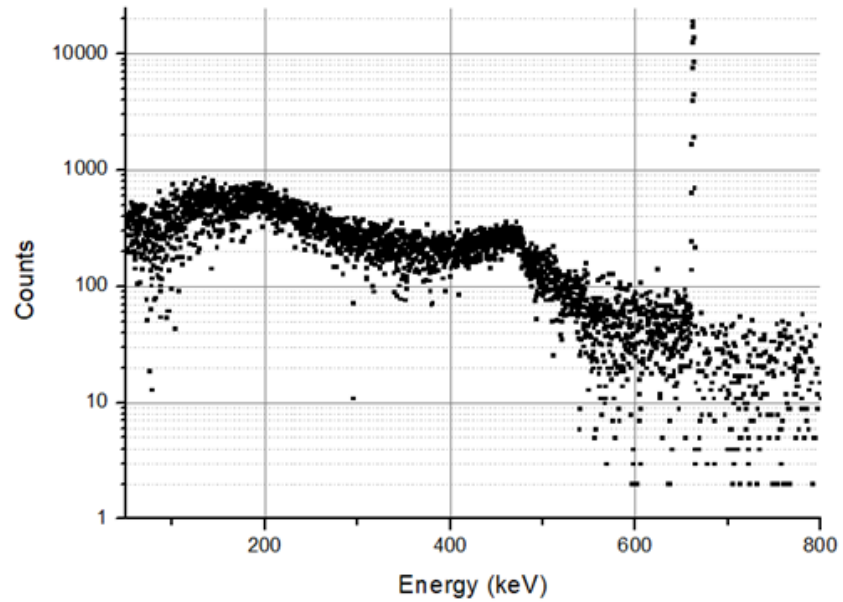
$$\lambda'_1 = \frac{\text{\# Counts of the Compton edge in the activated metallic slab}}{A(a)}$$

$$\lambda_2 = \frac{\text{\# Counts of the photopeak of the surface contamination for the metallic slab}}{A(c)}$$

$$\lambda'_2 = \frac{\text{\# Counts of the Compton edge of the surface contamination for the metallic slab}}{A(c)}$$

*A(a): known activity of activated metallic slab*

*A(c): known activity of surface contaminated metallic slab*



HPGe spectra from two different unknown sources representing the activated slab with surface contamination

	Volume activity $A(b)$	Surface activity $A'(b)$
<b>Nominal 1</b>	$4900 \pm 500$	$610 \pm 60$
<b>Experimental 1</b>	$4300 \pm 700$	$300 \pm 200$
<b>Nominal 2</b>	$2400 \pm 200$	$1500 \pm 150$
<b>Experimental 2</b>	$2500 \pm 300$	$1000 \pm 200$

# Conclusions

- The quantitative **agreement between the simulated and experimental spectrums** justifies the validity of the simulation method procedure for spectra production.
- The simulating spectra show that not only the gamma peaks are characteristic but also the continuum is representative for each source.
- Combination of gamma spectrometry measurements and MCNP simulation **allows distinguishing surface contamination from volume activation by the shape/ intensity or peak/ Compton ratio** of  $\gamma$ -spectra (of key nuclides  $^{137}\text{Cs}$  and  $^{60}\text{Co}$ ) analysis. This was checked by using  $\text{CeBr}_3$  and HPGe detectors for different known activity laboratory-made samples.
- The proposed method can be used for radiological characterization on activated reactor components.

**A non-destructive gamma spectrometry set-up designed for accurately characterizing  
low-activity metallic segments**

# Scope/ objective of the proposed set-up

## scope

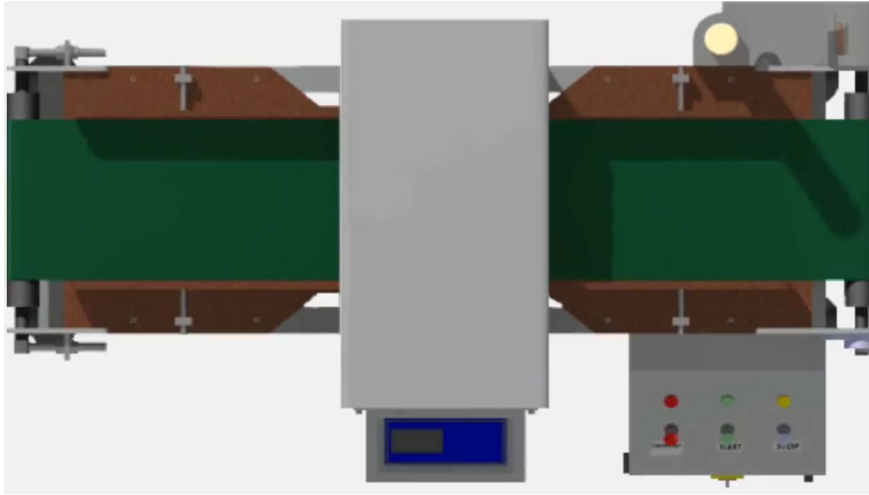
- The aim of this work is to crucially reduce the measurement uncertainty (less than 30 %), for measuring time comparable to that of the existing methods (i.e. 100kg, 2 min).
- To achieve adequate sensitivity ( i.e. 0.1 Bq/g) for the key radionuclides (Co-60, Cs-137) for acceptable measuring time

## objective

Measurement of low activity metallic waste at the stage after dismantling and cutting of components into segments to:

- decide if decontamination is worth
- select the appropriate decontamination techniques
- select the clearance methodology

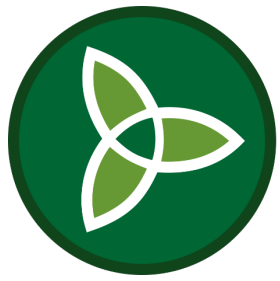
# The proposed measurement set-up



The metallic segments are put on a square shallow box.

Segments geometry	Total weight in the shallow box 1.2x1.2 m <sup>2</sup> (kg)
12 steel pipes of 0.1 m diameter, 0.002 m wall thickness, 1.2 m length	70
12 steel pipes of 0.1 m diameter, 0.003 m wall thickness, 1.2 m length	104
6 steel pipes of 0.2 m diameter, 0.003 m thickness, 1.2 m length	105
4 steel pipes of 0.3 m diameter, 0.003 m thickness, 1.2 m length	106
4 steel pipes of 0.3 m diameter, 0.004 m thickness, 1.2 m length	140
4 steel pipes of 0.3 m diameter, 0.01 m thickness, 1.2 m length	344
steel slab 1.2x1.2x0.02 m <sup>3</sup>	227
segments of small dimensions, homogeneous density of 4 Mg/m <sup>3</sup> , layer of 0.05 m thickness	291

total weight of steel segments of specific geometries



# PREDIS



## Development of new radiochemical procedures for DTM radionuclides

---

SUB-TASK 4.5.3

ANUMAIJA LESKINEN (VTT), MOJMÍR NĚMEC (CTU),  
TOMO SUZUKI (IMTA)



This project has received funding from the Euratom research and training programme 2019-2020 under grant agreement No 945098.

# Radiochemical approach



- Difficulty to measure directly **pure beta emitters** :
  - destructive method generally used.
- DTMs characterized by their **low energy emission**
- Evaluation of the activities by **scaling factors** to determine the activity level



- Development of a **radiochemical procedure** for the optimal detection and measurement in metallic sample
- **Highly selective** and efficient separation and purification
- Development of **sensitive** to **ultra-sensitive** method of measurement, depending on the radionuclide



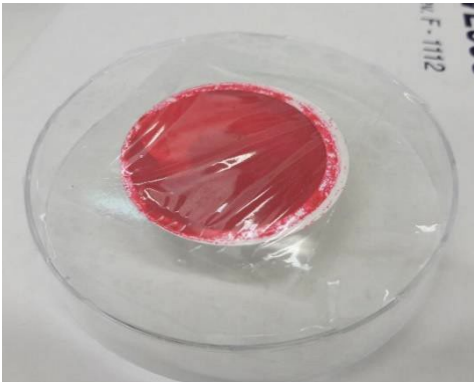
**$^{59,63}\text{Ni}$ ,  $^{41}\text{Ca}$ ,  $^{93}\text{Zr}$ ,  $^{93}\text{Mo}$**



- **Sample**
  - *Synthetic*: prepared in laboratory from chemical reagents
  - From *solid* containing the radionuclide source
  - *Surrogate* to simulate the radionuclide due to limited quantity or availability
- **Separation / Purification**
  - Purification by *chromatographic resins* to recover the radionuclide of interest
  - *Electrodeposition*
- **Conditioning**
  - Sample preparation for measurements
  - Liquid form or deposition on filters or on plates
- **Measurement**
  - Selection of an adapted analytical technique
  - Optimization of detection efficiency

## Innovation in sample preparation

$^{59,63}\text{Ni} \Rightarrow$  BEGe gamma spectrometry



Ni-DMG precipitate

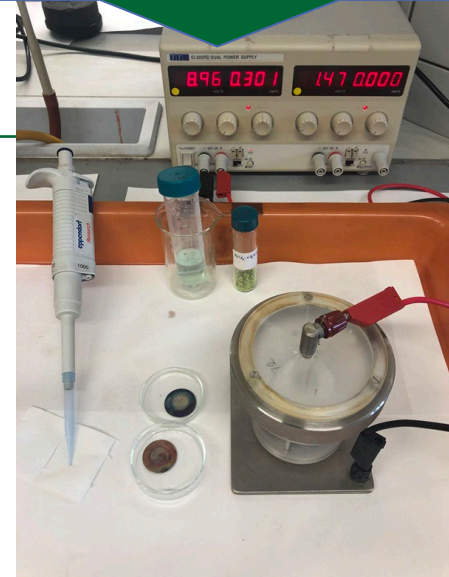


Direct evaporation on a membrane filter



Direct evaporation on a petri dish

$(^{59}+^{63})\text{Ni} \Rightarrow$  liquid scintillation (+ LE gamma)



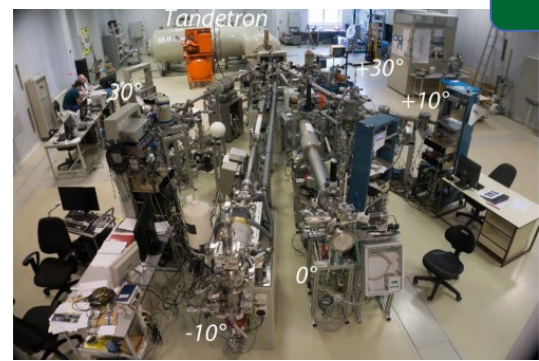
Electrodeposition



$^{93}\text{Zr} \Rightarrow$  liquid scintillation

Acid digestion of surrogate metallic samples

$^{41}\text{Ca} \Rightarrow$  AMS



$\text{CaF}_2 + \text{PbF}_2$  mixed sample preparation + ion mass selection



## Main challenges achieved

---

- Standard curves and calibration
  - Use of  $^{55}\text{Fe}$  standard for the measurements of  $^{59}\text{Ni}$  by BEGe spectrometry
    - Lowering the detection limits up to 20 Bq
    - Evaluation of  $^{60}\text{Co}$  effect as contaminant on  $^{55}\text{Fe}$  response: effect starting for activities at 200Bq of  $^{55}\text{Fe}$
  - Use of  $^{63}\text{Ni}$  standard for the measurements of  $^{93}\text{Zr}$  by liquid scintillation
    - Coupling chemical theory approach with experimental data
  - Selection of  $[\text{CaF}_3]^-$  and  $[\text{CaF}_4]^-$  ions for  $^{41}\text{Ca}$  assessment by MILEA AMS
- Optimization in sample preparations
  - Separation and purification of Ni and Zr using chromatographic resins from a complex solution (surrogate, radioactive)
  - Conditions achieved for efficient electrodeposition of Ni (Ni-63 with carrier) on planchette
- Validation in the MoNi intercomparison exercise 2024 (coordination VTT) with a high activity steel

# Intercomparison exercise on $^{59}\text{Ni}$ and $^{93}\text{Mo}$ analysis

- Collaboration with Nordic Nuclear Safety Research Program started in January 2024



- Nordic and Non-Nordic partners
- Project content:  $^{59}\text{Ni}$  and  $^{93}\text{Mo}$  analysis in highly activated steel. Other DTMs of interest  $^{55}\text{Fe}$ ,  $^{63}\text{Ni}$ ,  $^{93}\text{Zr}$ ,  $^{94}\text{Nb}$ . 2025 plan to focus on volatile DTMs e.g.  $^{14}\text{C}$ ,  $^{36}\text{Cl}$ ,  $^{79}\text{Se}$ .

## Partners so far



Norwegian University  
of Life Sciences



台湾電力公司  
Taiwan Power Company



Technical University  
of Denmark



*Thank you for your attention*





# PREDIS

**WP4: Innovations in metallic materials treatment and conditioning**

**T6 : Advances in encapsulation of materials in magnesium phosphate cements based matrices**

---

Céline Cannes (CNRS)

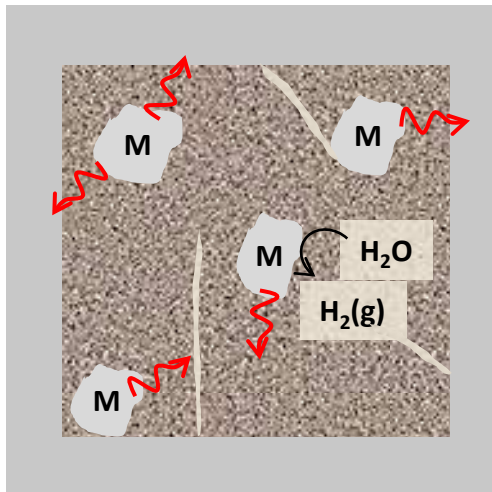
Contributors:

CEA, CNRS, CSIC, ENRESA, FZJ, IMT, KIPT, ORANO, POLIMI, RATEN, SCK CEN, UAM



This project has received funding from the Euratom research and training programme 2019-2020 under grant agreement No 945098.

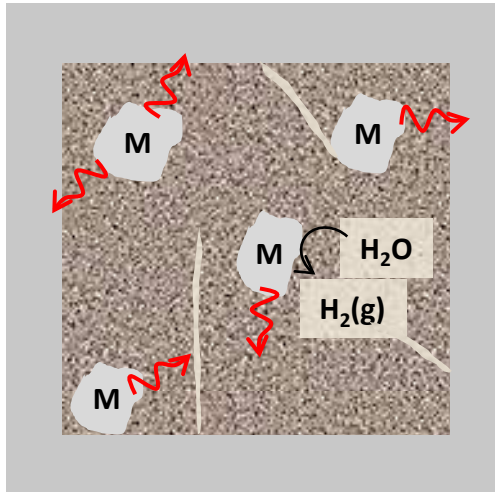
# Context



Main way to manage the low and intermediate level metallic waste:  
Encapsulation in cementitious matrices with a container made of steel or concrete.

- M: Low- or intermediate-level metal radioactive waste
- Conditioning in a cementitious matrix
- Container: steel or concrete

# Context



Main way to manage the low and intermediate level metallic waste:  
Encapsulation in cementitious matrices with a container made of steel or concrete.

conventional cementitious matrices:  
based on Portland cement or composite cements

- M: Low- or intermediate-level metal radioactive waste
- Conditioning in a cementitious matrix
- Container: steel or concrete

# Context

---

conventional cementitious matrices: Portland cement or composite cements

## Benefits

Low cost, easy supply

Process implemented at room temperature, no gas treatment

Good mechanical strength and self-shielding

Compatibility with aqueous waste

Good stability of well-designed cement matrices over time

Pore solution with a high pH allowing the precipitation of many radionuclides as hydroxides

# Context

---

conventional cementitious matrices: Portland cement or composite cements

## Benefits

- Low cost, easy supply
- Process implemented at room temperature, no gas treatment
- Good mechanical strength and self-shielding
- Compatibility with aqueous waste
- Good stability of well-designed cement matrices over time
- Pore solution with a high pH allowing the precipitation of many radionuclides as hydroxides

## Drawbacks

- Pore solution with a high pH causing the corrosion of some metallic radioactive waste (Al, Be)

# Context

---

conventional cementitious matrices: Portland cement or composite cements

## Benefits

- Low cost, easy supply
- Process implemented at room temperature, no gas treatment
- Good mechanical strength and self-shielding
- Compatibility with aqueous waste
- Good stability of well-designed cement matrices over time
- Pore solution with a high pH allowing the precipitation of many radionuclides as hydroxides

## Drawbacks

Pore solution with a high pH causing the corrosion of some metallic radioactive waste (Al, Be)



Need to define an acceptable alternative to calcium silicate cements for specific metal waste

# Objectives

---

## Al radioactive waste

Produced during the dismantling of old reactors.

Highly corroded in basic media.

## Be radioactive waste

Material of the Belgian Reactor 2 heart and in the ITER fusion facility.

Lack of data on the Be reactivity in cementitious media.

# Objectives

## Al radioactive waste

Produced during the dismantling of old reactors.

Highly corroded in basic media.

## Be radioactive waste

Material of the Belgian Reactor 2 heart and in the ITER fusion facility.

Lack of data on the Be reactivity in cementitious media.

## Steel

Material of the primary package drum.

More stable at basic pH than

In neutral pH media.

# Objectives

## Al radioactive waste

Produced during the dismantling of old reactors.

Highly corroded in basic media.

## Be radioactive waste

Material of the Belgian Reactor 2 heart and in the ITER fusion facility.

Lack of data on the Be reactivity in cementitious media.

## Steel

Material of the primary package drum.

More stable at basic pH than

In neutral pH media.

To fill an important gap for the management of LL and IL metallic radioactive waste (having high reactivity at high pH) by proposing magnesium phosphate cements (MPC) as alternative systems to conventional systems using Portland.

To control that the steel drum is not corroded in contact to the MPC.

# Guidelines of the study

---

## Magnesium phosphate cements (MPC)

New cement under consideration for conditioning radioactive metallic waste (having high reactivity at basic pH)

- Define MPC formulation based on WAC and economical considerations.
- Determine the behavior of MPC under leaching or irradiation.
- Study the corrosion of Al, Be (radioactive metal wastes) and steel (material of the primary package) in MPC.

## Objective: To optimize the MPC formulation

- Influence of MgO (hard-burned and reactive)
- Influence of the Mg/P ratio
- Influence of the water/(MgO + KH<sub>2</sub>PO<sub>4</sub>) ratio.
- Influence of the filler nature and the filler/(MgO + KH<sub>2</sub>PO<sub>4</sub>) ratio.
- Influence of MPC curing conditions
- Determination of the physical, chemical and mineralogical properties of the different MPCs

Increasing the MgO content increases the pH but, improves the mechanical strength and mitigates efflorescence.

A Mg/P molar ratio = 2 is recommended to improve mechanical properties and reduce the efflorescence.

Adding filler materials increased the amount of inert solid, can improve the workability and the mechanical strength.

Fillers are less expensive than MgO and  $\text{KH}_2\text{PO}_4$ . Their use can decrease the global cost of the material.

Volcanic ash shows good characteristics to be incorporated into MPC. However, its distribution and its homogeneity is not guaranteed.

The formulation should include the minimum amount of water (water/solid mass ratio 0.25) to generate K-struvite as the main product.

Absence of retarder leads to a rapid exothermic reaction, fast setting, and efflorescence. It is thus recommended to add a retarder. The type of retarder influences the fluidity of MPC.

Higher moisture content in the MPC allows higher instability due to the rapid dissolution of the phosphates excess at 1M M/P ratio.

The formation of K-struvite is complete under high moisture condition. The main ions content in the pore solution decreases to the formation of the main mineral phases, increasing the pore pH over time.

S ions were observed in pore solution (attributed to the FA). The presence of this ions leads to an increase of the pore pH.

In endogenous or isolated curing, the reaction does not progress completely due to the lack of water, with more dissolved ions in the pore solution and more unreacted products, showing more near neutral pH values.

Better pore network is observed at higher moisture content showing more capillary pores than in isolated condition, which improve the MPC stability.

Raw materials (MgO,  $\text{KH}_2\text{PO}_4$ , retarder, filler): high purity or from few providers

High cost of MPC = barrier to a larger industrial use

## Objective: To decrease the MPC cost

- MgO source
- Retarder
- Filler

Reactive MgO can be used to prepare MPC by using thiosulphate retarder alone (5 wt%) or in addition of boric acid (3wt% T + 2wt% HB) as retarders.

The setting time and the compressive strength values of these LC-MPC are in good agreement with the WAC.

The best compressive strength (53 MPa for a reactive MgO with 2wt.% HB and 3wt.% T) was obtained for a W/C of 0.5.

The hydration of MgO is enhanced, which leads to a better use of the raw material.

There is less efflorescence and the durability is better, as the depletion of  $\text{KH}_2\text{PO}_4$  is enhanced by the total hydration of high specific surface of reactive MgO.

When the filler FA is replaced by BFS, the content of K-struvite practically does not change.

MPC-BFS samples demonstrate the highest compressive strength compared to MPC-FA and MPC-FA-BFS samples.

The increased compressive strength values are explained by the presence of a denser structure of the MPC-BFS samples, in contrast to the structure of the MPC-FA and MPC-FA-BFS samples. This is due to the fact that BFS particles are more reactive compared to FA.

MPC: under consideration for radioactive metal waste immobilisation

→ It is primordial to study the leaching behavior of MPC

- Assess the behavior of MPC pastes/mortars under leaching by demineralized water (reference) and by an alkaline solution representative of the pore solution of conventional concrete placed in the near field of the cemented waste packages.
- Understand and model the degradation processes of the MPC matrix under well-controlled leaching conditions.

# ST6-3 leaching behavior of MPC

Following ANS 16.1 standard, leaching tests were carried out on MPC mortars prepared with different fillers, FA, BFS, or FA-BFS (50-50).

The leachability indices and diffusivities were calculated from their cumulative concentrations in the leachates. Whatever the filler, the leachability indices of K, Mg, P and B ( $LI > 9$ ) largely exceeded the LI index of 6 defined by the US Nuclear Regulatory Commission.

BFS was shown to be an interesting filler, leading to denser materials than FA, and thus allowing to slow down the release of elements in the leachates.

Leaching tests were performed on MPC (with FA) under semi-dynamic and well-controlled conditions (pH at 7 or 13.2, renewal of the leaching solution, N<sub>2</sub> atmosphere, and at 25°C).

At pH 7, leaching is mainly governed by diffusion of dissolved species through the pore network of the paste. An interface retreat of the solid is observed. K-struvite is fully dissolved close to the exposed surface of the samples. Then, in an intermediate zone, K-struvite coexists with cattite.

At pH 13.2, a layer of Ca-deficient hydroxyapatite (CDHA) rapidly forms on the surfaces and its thickness increases with the leaching duration. However, it is not sufficient to clog the porosity and protect the samples from further degradation. K-struvite dissolves near the exposed surface. In the intermediate zone, it mainly coexisted with brucite, CDHA and an hydrotalcite-like phase.

A first modeling approach based on reactive transport was proposed. Despite the simplified composition of the paste used for calculations, the model succeeded to reproduce the main mineralogical changes observed experimentally.

# ST6-4 Irradiation behaviour of MPC

MPC: under consideration for radioactive metal waste immobilisation

→ It is primordial to study the irradiation behavior of MPC

- Gamma irradiation: up to 200 kGy  $^{137}\text{Cs}$ , 400 Gy/h (IMT) and up to 1000 kGy  $^{60}\text{Co}$  2.5 kGy/h (POLIMI)
- $\text{H}_2$  production by micro-gas chromatography
- Compression tests
- Mineralogical and microstructural characterization (XRD, SEM-EDX and  $\mu\text{CT}$ )
- Leaching behavior of samples and leachate analysis (pH, conductivity, ion Chromatography and ICP)

# ST6-4 Irradiation behaviour of MPC

- ✓ No remarkable deterioration or changes were observed for cumulative doses up to 1000 kGy.
- ✓ Results show the good resistance of fresh matrix to irradiation.
- ✓ The WACs are respected regarding leaching and compression tests for MPC samples after irradiation.
- ✓ The MPC matrix characterisation supports experimental evidences.

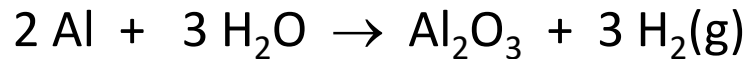
Magnesium phosphate cement represents a promising immobilisation matrix for radioactive reactive metal wastes.

# ST6-5 Al corrosion in MPC

$4 < \text{pH}$  or  $\text{pH} > 9$ : high corrosion of Al



$4 < \text{pH} < 9$  : passivation of Al by solid phase



High risk of Al corrosion in OPC ( $\text{pH} > 12.6$ ) with  $\text{H}_2$  release.  
Risk of radionuclides release and matrix degradation

## Test of MPC and alternative Portland binders to condition Al radioactive waste

- Study the Al corrosion in MPC and comparison with the corrosion in CEM I.
- Determine the volume of  $\text{H}_2$  released.
- Determine the effect of resaturation of the mortars on the Al reactivity.

# ST6-5 Al corrosion in MPC

The Al corrosion is the lowest in MPC and acceptable in CEM I + Silica fume. They both constitute good alternatives to CEM I.

The lowest Al corrosion was measured in MPC with a  $\text{MgO}/\text{KH}_2\text{PO}_4$  ratio around 2M (pore pH 7 - 9).

The pore moisture content does affect the Al corrosion kinetic.

The alkalisation of MPC matrix reactivate the Al corrosion by increasing the pore water solution pH.

Al is less corroded in low-cost MPC prepared with reactive MgO and thiosulphate: lower  $\text{H}_2$  release was measured.

LPR & EIS method gave similar  $\text{H}_2$  assessment values. These results confirm the possibility to use both methods to study the corrosion of a metal encapsulated in a cementitious matrix.

MPC: good alternative for AI radioactive waste immobilisation by reducing the pH of the pore water solution.

## What about the reactivity of C-steel, material used as the primary waste package?

- Study the C-steel corrosion in MPC and comparison with the corrosion in CEM I.
- Determine the volume of H<sub>2</sub> released.
- Determine the effect of MPC formulation.

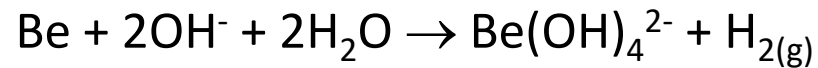
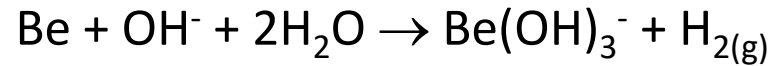
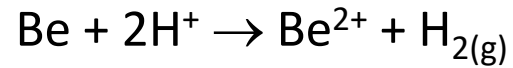
# ST6-6 Steel corrosion in MPC

The reactivity of C-steel in MPC is similar to that in OPC with the only difference that initially the corrosion rate is higher in MPC and towards the end of the test it decreased while in OPC it is the opposite.

C-steel is significantly corroded in low cost MPC compared to the reference MPC. Differences of reactivity in the LC-MPC prepared with only thiosulphate as retarder (B0T5) or with a mixture of thiosulphate and boric acid (B2T3) are minimal. However, the overall impedance of LC-MKPC formulations increases with prolonged exposure, suggesting a potential enhancement in corrosion resistance.

To overcome the higher corrosion of steel, concrete drums can be used for AI embedding in low cost MPC. In cases the steel corrosion in the presence of thiosulphate exhibits linear kinetic corrosion, the consideration of concrete drums over steel ones could be warranted. The decrease in the cost of cement manufacturing could offset the high cost of concrete drums compared to steel drums.

Acid or high basic pH: high corrosion of Be



High risk of Be corrosion at high basic pH with H<sub>2</sub> release.

Risk of radionuclides release and matrix degradation

Neutral pH: passivation of Be by a solid phase



### Be corrosion (rate and mechanism) in MPC and comparison with Portland cement based matrix

- Electrochemical measurements.
- H<sub>2</sub> volume measurement by gas chromatography.
- Gravimetry.
- Scanning electron microscopy and X-ray diffraction.

In high basic pH solutions (pH 12.5-14), the corrosion rate increases exponentially with pH. At pH ~13.5, the corrosion rate reaches ~2  $\mu\text{m}/\text{y}$  after 120 to 365 days of immersion. The Be surface reveals pitting corrosion and a thin corrosion product layer. Mechanical defects on the initial Be surface acts as the initiation places for pitting corrosion.

In near neutral pH solutions, pure beryllium corrodes slower (0.04 to 1.4  $\mu\text{m}/\text{y}$ ) than the S-200-F grade (~12  $\mu\text{m}/\text{y}$ ). The addition of boric acid helps decreasing the corrosion rate. SEM analysis reveals the presence of  $\text{KBePO}_4 \cdot \text{H}_2\text{O}$  crystals at the surface of both metal grade after corrosion in MPC solution.

The corrosion rates are lower in matrices than in solutions: 0.1  $\mu\text{m}/\text{y}$  in OPC and 0.05  $\mu\text{m}/\text{y}$  in MPC.

The comparison of the corrosion of Be embedded in MPC and LC-MPC was difficult as the results obtained in LC-MPC were not reproducible. Extra tests are therefore needed to better understand the results.

SEM analysis confirms the little corrosion rate as no corrosion product layer was observed. However, needle-like particles were observed in the OPC close to the Be surface.

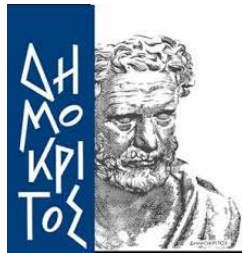
# Thanks for your attention!





# PREDIS

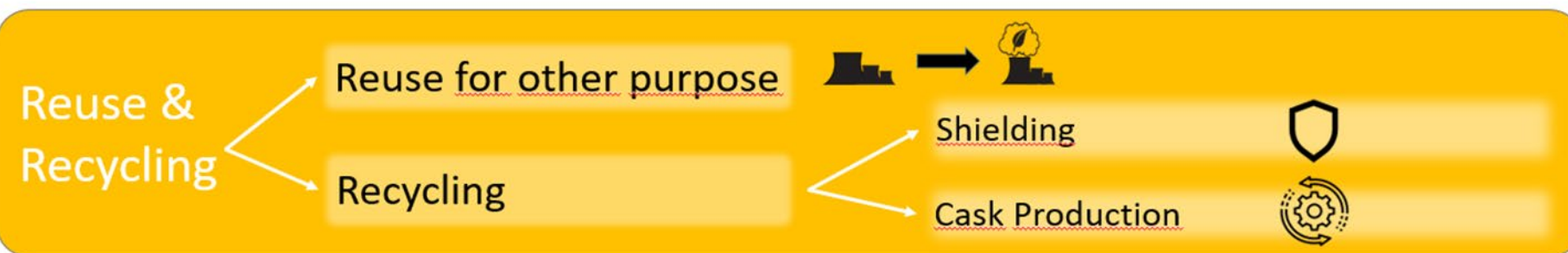
## **A non-destructive gamma spectrometry set-up for characterization of low activity metallic waste**



D. Mavrikis and A. Savidou,  
NCSR

# Metallic waste management routes

Mech./ chem. decontamination & clearance



Disposal as radioactive waste

# Scope/ objective of the proposed set-up

## scope

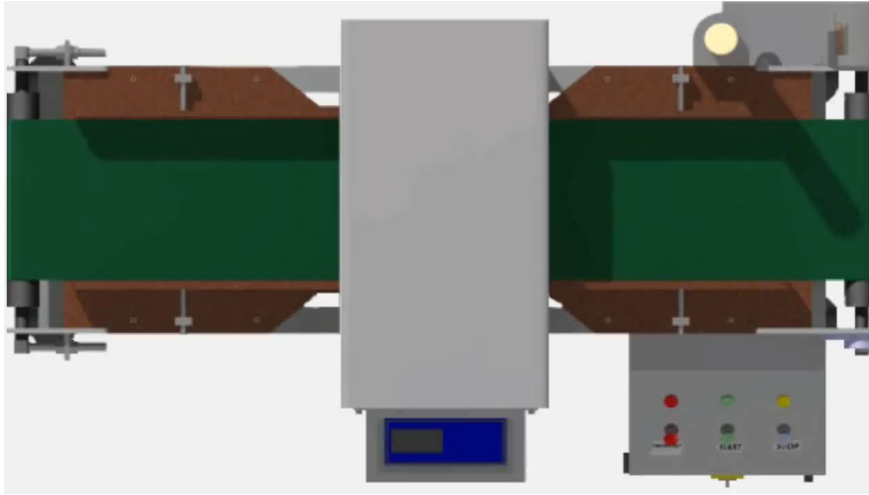
- The aim of this work is to crucially reduce the measurement uncertainty (less than 30 %), for measuring time comparable to that of the existing methods (i.e. 100kg, 2 min).
- To achieve adequate sensitivity ( i.e. 0.1 Bq/g) for the key radionuclides (Co-60, Cs-137) for acceptable measuring time

## objective

Measurement of low activity metallic waste at the stage after dismantling and cutting of components into segments to:

- decide if decontamination is worth
- select the appropriate decontamination techniques
- select the clearance methodology

# The proposed measurement set-up



The metallic segments are put on a square shallow box.

Segments geometry	Total weight in the shallow box 1.2x1.2 m <sup>2</sup> (kg)
12 steel pipes of 0.1 m diameter, 0.002 m wall thickness, 1.2 m length	70
12 steel pipes of 0.1 m diameter, 0.003 m wall thickness, 1.2 m length	104
6 steel pipes of 0.2 m diameter, 0.003 m thickness, 1.2 m length	105
4 steel pipes of 0.3 m diameter, 0.003 m thickness, 1.2 m length	106
4 steel pipes of 0.3 m diameter, 0.004 m thickness, 1.2 m length	140
4 steel pipes of 0.3 m diameter, 0.01 m thickness, 1.2 m length	344
steel slab 1.2x1.2x0.02 m <sup>3</sup>	227
segments of small dimensions, homogeneous density of 4 Mg/m <sup>3</sup> , layer of 0.05 m thickness	291

total weight of steel segments of specific geometries

# The proposed measurement set-up

- MCNPX simulations were carried out for source-detector configuration and the models were validated by using volume sources
- 3"×3" NaI(Tl) (reference detector) & HPGe detector (20%) were simulated



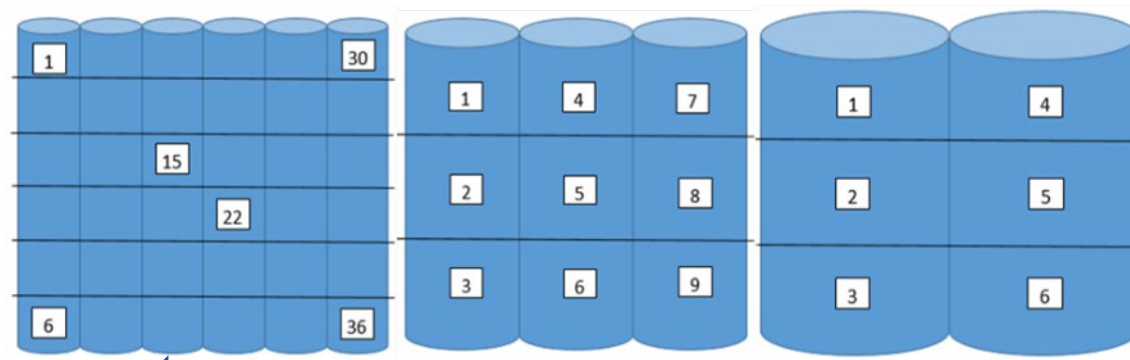
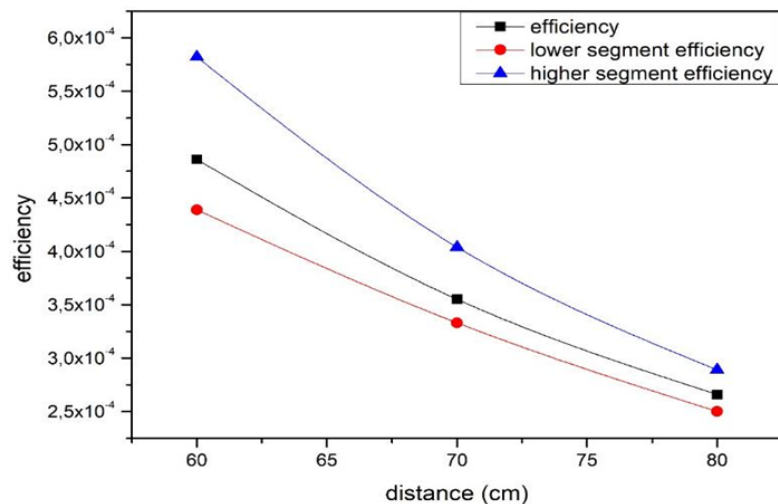
- Volume sources representing metallic segments of pipes and slabs with  $^{137}\text{Cs}$  contamination were prepared and used for validation of the MCNPX models
- Surface contamination of the volume sources was  $0.94 \pm 0.09 \text{ Bq/cm}^2$

# Optimum measurement distance

## Pipes – NaI(Tl) detector

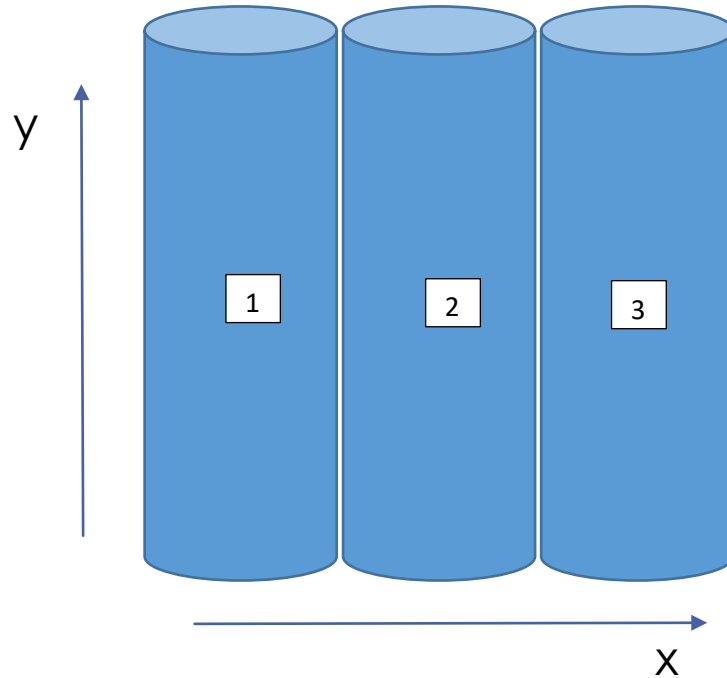
- 20 cm diameter
- $^{137}\text{Cs}$  internal contamination

- *detection efficiency for homogeneous activity distribution*
- *Study of activity inhomogeneity. Lower and the higher efficiency segment*



← bias due to the activity inhomogeneity is lower when the distance of detector from the bottom of the shallow box is greater

# Missing segments (half-full box)



Pipe diameter = 20 cm  
 Pipe thickness = 0.3 cm  
 Pipe Length = 60 cm

## CASE I

- a) pipes 1 and 3 are homogeneously contaminated, pipe 2 is not contaminated
- b) pipes 1 and 3 are homogeneously contaminated, pipe 2 is missing

## CASE II

- a) pipes 1 and 2 are homogeneously contaminated, pipe 3 is not contaminated
- b) pipes 1 and 2 are homogeneously contaminated, pipe 3 is missing

	Efficiency (a)	Efficiency (b)	Efficiency (three pipes)
CASE I	$2.63 \times 10^{-4}$	$2.62 \times 10^{-4}$	$2.66 \times 10^{-4}$
CASE II	$2.67 \times 10^{-4}$	$2.68 \times 10^{-4}$	

***Missing segments has no significant effect to the measurement efficiency***

# Detection efficiency and expected MDA

## Pipes – HPGe detector

- homogeneous contamination on the internal surface of steel pipes,
- Efficiency of each HpGe detector 20%

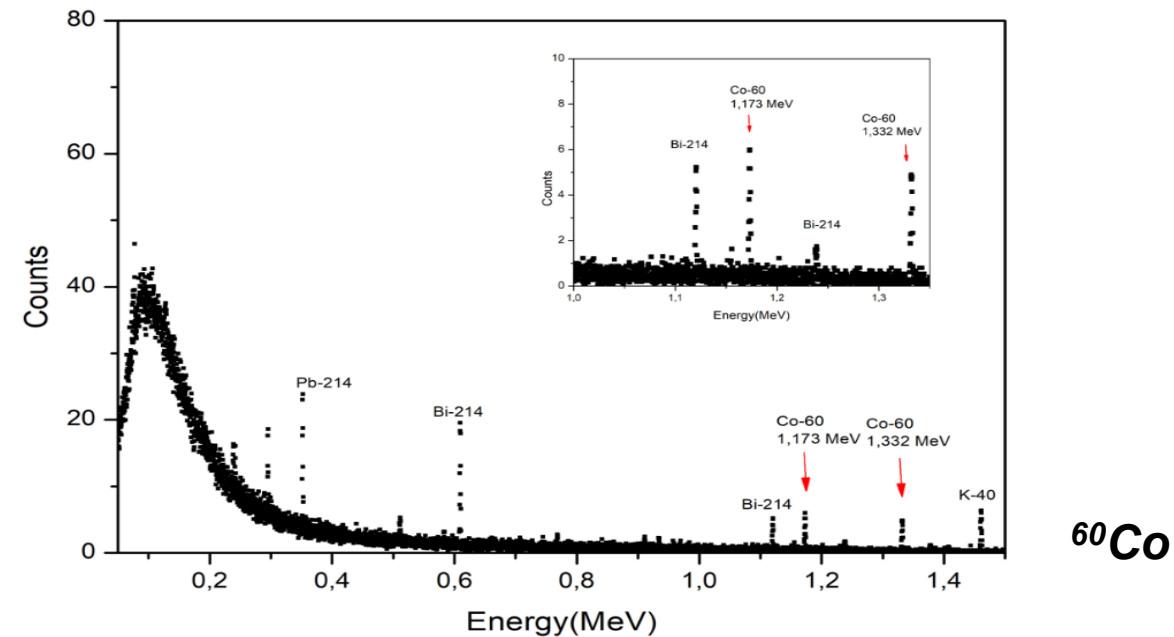
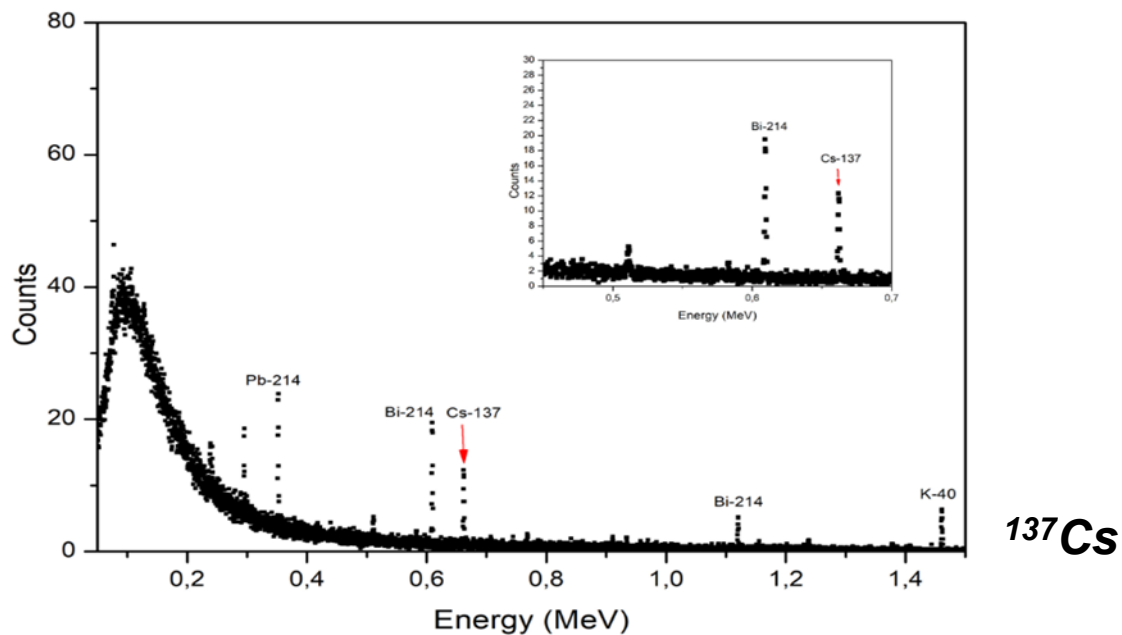
Pipes diameter (cm)	Total weight (kg)	Efficiency	MDA <sup>137</sup> Cs in Bq/g		
			area of low background		
			2 min	5 min	8 min
10	26.00	$5.0 \times 10^{-5}$	0.08	0.05	<b>0.04</b>
20	26.25	$5.59 \times 10^{-5}$	0.07	0.05	<b>0.04</b>
30	26.50	$6.48 \times 10^{-5}$	0.06	0.04	<b>0.03</b>

MCNPX detection efficiencies for homogeneous activity distribution of <sup>137</sup>Cs as well as the expected MDA

Pipes diameter (cm)	Total weight (kg)	Efficiency	MDA <sup>60</sup> Co in Bq/g		
			area of low background		
			2 min	5 min	8 min
10	26.00	$1.7 \times 10^{-5}$	0.21	0.13	<b>0.10</b>
20	26.25	$1.88 \times 10^{-5}$	0.19	0.11	<b>0.09</b>
30	26.50	$2.17 \times 10^{-5}$	0.16	0.10	<b>0.08</b>

MCNPX detection efficiencies for homogeneous activity distribution of <sup>60</sup>Co as well as the expected MDA

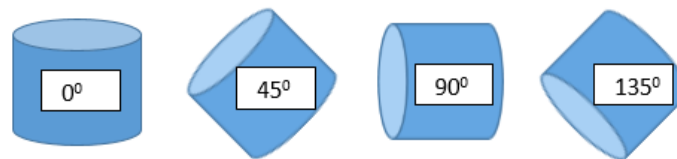
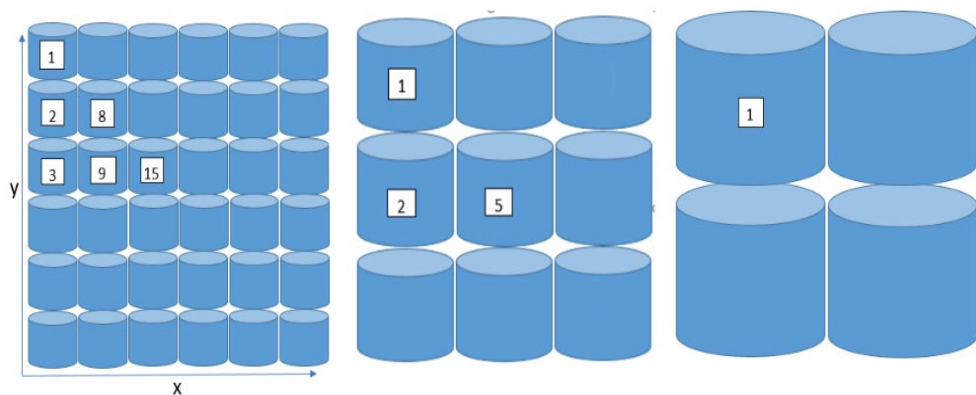
# Simulating spectra



*The spectrum resulting from the summation of:*

- 4 MCNPX spectra (4 HPGe detectors 20% ), popes of 10 cm diameter with 0.1 Bq/g homogeneous activity, measured for 2 min simultaneously*
- the background spectrum for 8 min at area of low background.*

# Direction of segments (convex pipes)



- *HPGe*
- rotations of 0°, 45°, 90°, 135° with respect to (x, y)

Diameter (cm)	Efficiency	Bias (act. inhomog.)	Bias (act. inhomog. & direction)
10	$5.00 \times 10^{-5}$	-12% to +11%	-13% to +11%
20	$5.60 \times 10^{-5}$	-6% to +14%	-6% to +14%
30	$6.49 \times 10^{-5}$	-3% to +9%	-3% to +9%

homogeneous activity distribution  $^{137}\text{Cs}$

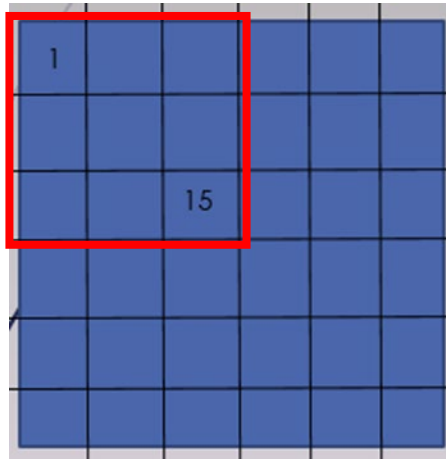
Diameter r (cm)	Efficiency	Bias (act. inhomog.)	Bias (act. inhomog. & direction)
10	$1.70 \times 10^{-5}$	-14% to +13%	-15% to +14%
20	$1.88 \times 10^{-5}$	-3% to +14%	-5% to +14%
30	$2.18 \times 10^{-5}$	-2% to +10%	-2% to +10%

homogeneous activity distribution  $^{60}\text{Co}$  (1.17MeV)

**Direction of segments has no significant effect to the measurement efficiency**

# Slabs

- HPGe detector 20% metallic square slab of 60 cm side
- $^{137}\text{Cs}$  &  $^{60}\text{Co}$  homogeneous surface contamination

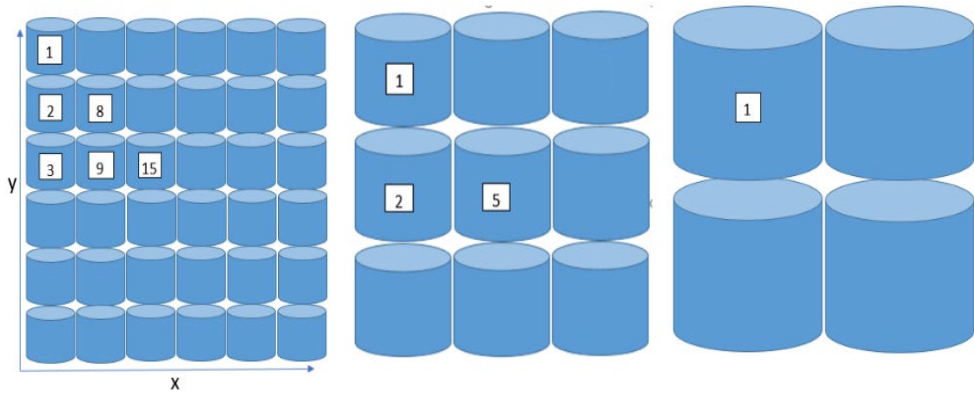


36 square segments to study the activity inhomogeneity

	Efficiency homog.	Bias
$^{137}\text{Cs}$	$6.0 \times 10^{-5}$	-10% to 10%
$^{60}\text{Co}$ (1.17 MeV)	$1.89 \times 10^{-5}$	-12% to 10%

overall detection efficiency and the respective bias (segment 1 & 15)

# Validation of the MCNP models



Pipes of 10,20,30 cm diameter & numbered segments



Experimental verification of evaluated by MCNPX detection efficiencies

Object of measurement	Detector	Efficiency by MCNP	Efficiency by measurement	
pipe of 20 cm diameter: segments 1,2,3	HPGe 20%	$5.47 \times 10^{-5}$	$5.43 \times 10^{-5}$ , 4%	-0.7%
pipe of 30 cm diameter, segments 1,2	HPGe 20%	$6.45 \times 10^{-5}$	$5.87 \times 10^{-5}$ , 4%	-9 %
pipe of 30 cm diameter, segments 1	HPGe 20%	$6.45 \times 10^{-5}$	$6.33 \times 10^{-5}$ , 6%	-2%
pipe of 30 cm diameter, segments 1	HPGe 20%	$6.45 \times 10^{-5}$	$5.75 \times 10^{-5}$ , 6%	-11%
pipe of 10 cm diameter, segments 1-6	HPGe 20%	$4.78 \times 10^{-5}$	$5.06 \times 10^{-5}$ , 4%	+6%
pipe of 20 cm diameter, segments 4,5,6	3x3 NaI(Tl)	$2.72 \times 10^{-4}$	$2.82 \times 10^{-4}$	+4%
pipe of 30 cm diameter, segments 1,2	3x3 NaI(Tl)	$3.10 \times 10^{-4}$	$2.85 \times 10^{-4}$	-8%
slab 0.6x0.6 m <sup>2</sup>	3x3 NaI(Tl)	$2.80 \times 10^{-4}$	$3.00 \times 10^{-4}$	+7%

*Evaluated by MCNPX detection efficiencies for 3"×3" NaI(Tl) & HPGe 20% detectors for specific metallic segments are compared with the respective experimentally determined efficiencies*

# Conclusions

The results showed that by the proposed set-up based on HPGe 20% detectors:

- crucial reduction of the measurement uncertainty (less than 25%) of metallic waste can be achieved
- sufficient measurement sensitivity (determination of 0.1 Bq/g of the key radionuclides  $^{137}\text{Cs}$  and  $^{60}\text{Co}$  in metallic waste of total mass more than 100 kg can be achieved in less than 2 min).

the proposed set-up for measurement of metallic waste after decommissioning can be used to select the management route as well as the decontamination and clearance procedure



**PREDIS**

**Thank you!!**



# PREDIS



## Development of decontamination process for metallic radioactive effluents

---

**MATHURIN ROBIN**

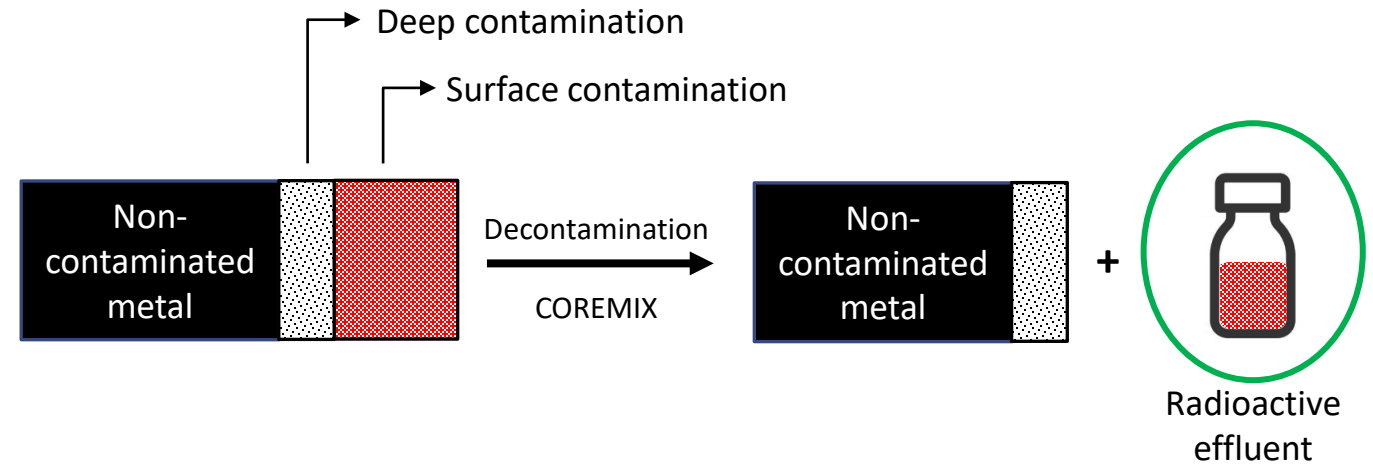
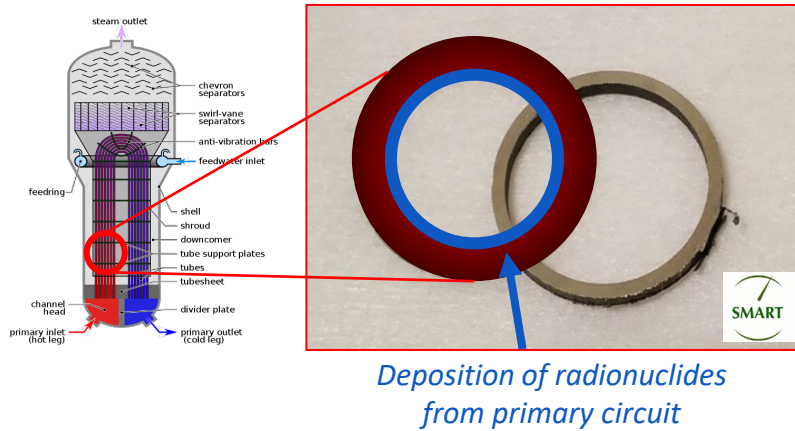
**TOMO SUZUKI, ABDESSELAM ABDELOUAS, MARCEL MOKILI**



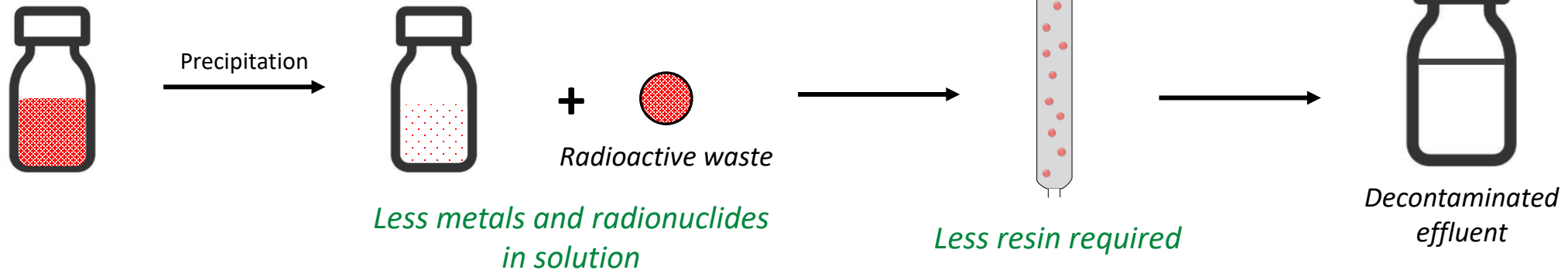
This project has received funding from the Euratom research and training programme 2019-2020 under grant agreement No 945098.

# Introduction

## Context

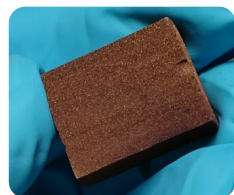


## Objectives



## COREMIX process

Stainless Steel 316

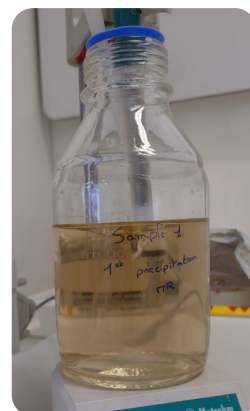
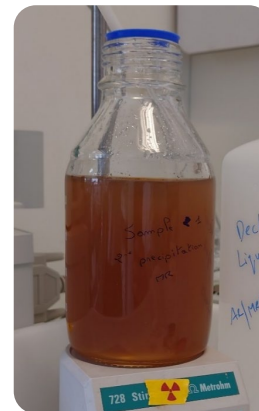


Ni-alloy 600

KMnO<sub>4</sub> step  
15 mM / 80°C / 3hH<sub>2</sub>C<sub>2</sub>O<sub>4</sub> step  
18.5 mM / 80°C / 3h

Radioactive effluent

## Precipitation process

Oxalic acid destruction step  
0.1 M H<sub>2</sub>O<sub>2</sub> / 80°C / 24h1<sup>st</sup> precipitation  
pH 8.52<sup>nd</sup> precipitation  
pH 12

Filtration



Decontaminated effluent



Contaminated sludge

# Results

## ➤ Decontamination by COREMIX process

- 4 cycles
- 350 mL of effluents
- Total activity of  $24.5 \pm 1.4$  kBq/g



## ➤ Activity mainly coming from $^{55}\text{Fe}$ , $^{60}\text{Co}$ and $^{63}\text{Ni}$ (24h counting time)

- Initial activity  $\approx 28\,000$  Bq/L
- Final activity  $\approx 36$  Bq/L

✓ **DF  $\approx 800$**

	Activity before treatment (Bq/L)	Activity after treatment (Bq/L)	DF
$^{54}\text{Mn}$	$73 \pm 29$	$< 0.7^*$	$> 60$
$^{55}\text{Fe}$	$5\,200 \pm 1\,200$	$28 \pm 8$	$190 \pm 100$
$^{60}\text{Co}$	$15\,300 \pm 1\,100$	$4.8 \pm 0.7$	$3\,200 \pm 700$
$^{63}\text{Ni}$	$7\,300 \pm 1\,800$	$< 0.8^*$	$> 6\,900$
$^{99}\text{Tc}$	$124 \pm 44$	$< 0.3^*$	$> 270$
$^{125}\text{Sb}$	$94 \pm 38$	$< 1.8^*$	$> 32$
<b><u>Total :</u></b>	<b><math>28\,100 \pm 4\,200</math></b>	<b><math>36 \pm 9</math></b>	<b><math>780 \pm 310</math></b>

\*The measured values are below the detection limit of the equipment.

# Summary



## ➤ Optimisation of the precipitation process

- pH
- Oxalic acid destruction
- Time of contact
- Reagents -> NaOH / Na<sub>2</sub>S / Na<sub>3</sub>PO<sub>4</sub>

## ➤ Characterisation

- pH 8.5 -> Fe(OH)<sub>3</sub> / FeO(OH)
- pH 12 -> Mn<sub>3</sub>O<sub>4</sub>

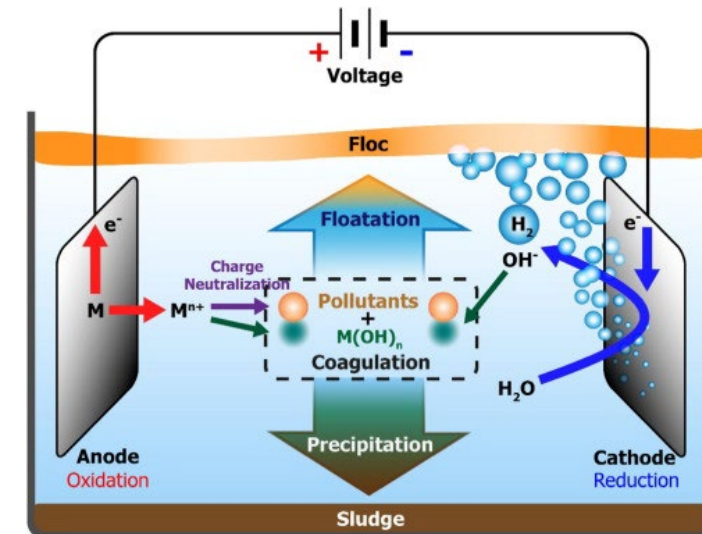
## ➤ Application

- Functional on SS316 and A600 effluent
- Effective on more than 20 elements
- DF of 800
- 99% less resin required



## ➤ Precipitation by electrocoagulation

- Avoid the use of precipitant
- Increasing efficiency
- Reduce the amount of salts in the effluent



Picture taken from :  
Chunjiang, A, 2017

## Contact information

- **robin@subatech.in2p3.fr;**
- SUBATECH (IMT Atlantique, CNRS/IN2P3, Université de Nantes), BP 20722, 44307 Nantes Cedex 3, France

